MINISTÉRIO DA EDUCAÇÃO
UNIVERSIDADE FEDERAL DO RIO GRANDE DO SUL
PROGRAMA DE PÓS-GRADUAÇÃO EM ENGENHARIA MECÂNICA

ON A CONTINUOUS ENERGY MONTE CARLO SIMULATOR FOR NEUTRON INTERACTIONS IN REACTOR CORE MATERIAL CONSIDERING UP-SCATTERING EFFECTS IN THE THERMAL ENERGY REGION

by

Luiz Felipe Fracasso Chaves Barcellos

Dissertação para obtenção do Título de
Mestre em Engenharia

Porto Alegre, February 2016.

SOBRE UM SIMULADOR MONTE CARLO DE ENERGIA CONTÍNUA PARA INTERAÇÕES NEUTRÔNICAS NO MATERIAL DO NÚCLEO DE REATOR CONSIDERANDO EFEITOS DE *UP-SCATTERING* NA REGIÃO DE ENERGIAS TÉRMICAS

por

Luiz Felipe Fracasso Chaves Barcellos

Engenheiro Mecânico

Dissertação submetida ao Corpo Docente do Programa de Pós-Graduação em Engenharia Mecânica, PROMEC, da Escola de Engenharia da Universidade Federal do Rio Grande do Sul, como parte dos requisitos necessários para a obtenção do Título de

Mestre em Engenharia

Área de Concentração: Fenômenos de Transporte

Orientador: Prof. Dr. Bardo Ernst Josef Bodmann

Aprovada por:

Prof. Dr. Sérgio Queiroz Bogado Leite ..... ELETRONUCLEAR

Prof. Dr. Fábio Souto de Azevedo ..... PPGMAp - UFRGS

Prof. Dr. Volnei Borges ..... PROMEC - UFRGS

Prof. Dr. Luiz Alberto Oliveira Rocha
Coordenador do PROMEC

Porto Alegre, 25 de Fevereiro de 2016.

ACKNOWLEDGEMENTS

I thank CAPES for the financial support during the master's degree. I am also thankful to Universidade Federal do Rio Grande do Sul for the study opportunity.

I also thank the members of the evaluation board, Prof. Dr. Sérgio Queiroz Bogado Leite, Prof. Dr. Fábio Souto de Azevedo and Prof. Dr. Volnei Borges for the paramount contributions during the review of this work.

A special thank you to my professor advisor Prof. Dr. Bardo Ernst Josef Bodmann as well as to Prof. Dr. Marco Túlio de Vilhena for their treasured counselling and friendship.

Finally I would like to thank all my friends and family for their esteemed support.

RESUMO

Neste trabalho o transporte de nêutrons é simulado em materiais presentes no núcleo de reatores. O espectro de nêutrons é decomposto como uma soma de três distribuições de probabilidade. Duas das distribuições preservam sua forma com o tempo, mas não necessariamente sua integral. Uma das duas distribuições é devido ao espectro de fissão, isto é, altas energias de nêutrons, a outra é uma distribuição de Maxwell-Boltzmann para nêutrons de baixas energias (térmicos). A terceira distribuição tem uma forma a priori desconhecida e que pode variar com o tempo, sendo determinada a partir de uma simulação Monte Carlo com acompanhamento dos nêutrons e suas interações com dependência contínua de energia. Isto é obtido pela parametrização das seções de choque dos materiais do reator com funções contínuas, incluindo as regiões de ressonâncias resolvidas e não resolvidas. O objetivo deste trabalho é implementar efeitos de *up-scattering* através do tratamento estatístico da população de nêutrons na distribuição térmica. O programa de simulação calcula apenas *down-scattering*, pois o cálculo do *up-scattering* microscópico aumenta significativamente tempo de processamento computacional. A fim de contornar esse problema, pode-se reconhecer que *up-scattering* é dominante na região de energia mais baixa do espectro, onde assume-se que as condições de equilíbrio térmico para nêutrons imersos em seu ambiente são válidas. A otimização pode, assim, ser atingida pela manutenção do espectro de Maxwell-Boltzmann, isto é, *up-scattering* é simulado por um tratamento estatístico da população de nêutrons. Esta simulação é realizada utilizando-se dependência energética contínua, e, como um primeiro caso a ser estudado assume-se um regime recorrente. As três distribuições calculadas são então utilizadas no código Monte Carlo para calcular os passos Monte Carlo subsequentes.

Palavras-chave: Transporte de Nêutrons, Probabilidades de Interação, Método de Monte Carlo, Distribuições Espectrais de Probabilidade, Regime Recorrente.

ABSTRACT

In this work the neutron transport is simulated in reactor core materials. The neutron spectrum is decomposed as a sum of three probability distributions. Two of the distributions preserve shape with time but not necessarily the integral. One of the two distributions is due to prompt fission, i.e. high neutron energies and the second a Maxwell-Boltzmann distribution for low (thermal) neutron energies. The third distribution has an a priori unknown and possibly variable shape with time and is determined from a Monte Carlo simulation with tracking and interaction with continuous energy dependence. This is done by the parametrization of the material cross sections with continuous functions, including the resolved and unresolved resonances region. The objective of this work is to implement up-scattering effects through the treatment of the neutron population in the thermal distribution. The simulation program only computes down-scattering, for the calculation of microscopic up-scattering increases significantly computational processing time. In order to circumvent this problem, one may recognize that up-scattering is dominant towards the lower energy end of the spectrum, where we assume that thermal equilibrium conditions for neutrons immersed in their environment holds. The optimization may thus be achieved by the maintenance of the Maxwell-Boltzmann spectrum, i.e. up-scattering is simulated by a statistical treatment of the neutron population. This simulation is performed using continuous energy dependence, and as a first case to be studied we assume a recurrent regime. The three calculated distributions are then used in the Monte Carlo code to compute the Monte Carlo steps with subsequent updates.

Keywords: Neutron Transport, Tracking and Interaction Probabilities, Monte Carlo Method, Spectral Probability Distributions, Recurrent Regime.

CONTENTS

LIST OF FIGURES

LIST OF TABLES

LIST OF ACRONYMS ANS ABBREVIATIONS

CAPES	Coordenação de Aperfeiçoamento de Pessoal de Nível Superior
PROMEC	Programa de Pós-Graduação em Engenharia Mecânica
UFRGS	Universidade Federal do Rio Grande do Sul

LIST OF SYMBOLS

A	Atomic mass, $a.m.u$ or $^{g}/_{moles}$
dx	Differential thickness, m
e	Enrichment of uranium dioxide
E	Energy, MeV
f	Fission reaction
${}^{4}_{2}He^{+2}$	Alpha particle
I	Mono-energetic neutron beam, $^{neutrons}/_{m^2\,s}$
k_B	Boltzmann constant, $8.6173 \times 10^{11}\ MeV/K$
L	Total length travelled by the neutron, cm
m_k	Number of neutrons emitted by reaction "k"
M	Molecular weigh, $^{g}/_{moles}$
n	neutron
$n(\vec{r}, \vec{\Omega}, E, t)$	Neutron density, $^{neutrons}/_{cm^3}$
N	Atomic density, $^{atoms}/_{m^3}$
N_{235}	Atomic density of U-235, $^{atoms}/_{m^3}$
N_{238}	Atomic density of U-238, $^{atoms}/_{m^3}$
N_A	Avogrado number, $^{atoms}/_{moles}$
$\vec{r}$	Position vector in the Cartesian system
p	Proton
p_i	Percentage of S travelled in region "i"
Q	Excitation energy of target nucleus
r	Weight percentage
R	Reaction rate per square meter, $^{reactions}/_{m^2\,s}$
S	Multiple of mean free path
t	time, s
T	temperature, K
v	Absolute value of the velocity vector, $^{m}/_{s}$

v_{CM}	Center of mass speed, $^{m}/_{s}$
$v_{CM,1}$	Neutron speed in the center of mass system before the collision, $^{m}/_{s}$
$v_{CM,1}^{'}$	Neutron speed in the center of mass system after the collision, $^{m}/_{s}$
$v_{CM,2}$	Nucleus speed in the center of mass system before the collision, $^{m}/_{s}$
$v_{CM,2}^{'}$	Nucleus speed in the center of mass system after the collision, $^{m}/_{s}$
$v_{Lab,1}$	Neutron speed in the laboratory system before the collision, $^{m}/_{s}$
$v_{Lab,1}^{'}$	Neutron speed in the laboratory system after the collision, $^{m}/_{s}$
$v_{Lab,2}$	Nucleus speed in the laboratory system before the collision, $^{m}/_{s}$
$v_{Lab,2}^{'}$	Nucleus speed in the laboratory system after the collision, $^{m}/_{s}$
α	Angle in the spherical system, *radians*
β	Angle in the spherical system, *radians*
γ	Gamma radiation
θ	Angle in the spherical system, *radians*
λ	Mean free path, m
ν	Average fission neutrons
ρ	Density, $^{kg}/_{m^3}$
σ	Microscopic cross section, *barns*
σ_a	Microscopic absorption cross section, *barns*
σ_s	Microscopic scattering cross section, *barns*
σ_t	Microscopic total cross section, *barns*
Σ_k	Macroscopic cross section of reaction "k", cm^{-1}
Σ_t	Total macroscopic cross section, cm^{-1}
ϕ	Neutron flux, $^{neutrons}/_{cm^2\,s}$
Φ	Angle in the spherical system, *radians*
$\chi_f(E)$	Prompt fission spectrum
ψ	Angle in the spherical system, *radians*
$\vec{\Omega}$	Direction vector in the spherical system
$\vec{\Omega}'$	Direction vector in the spherical system
$\vec{\Omega}_f$	Final neutron direction vector
$\vec{\Omega}_f^*$	Generalized final direction vector
$\vec{\Omega}_i$	Initial neutron direction vector

$\vec{\Omega}_P$	Auxiliary direction vector
$\vec{\Omega}_Q$	Auxiliary direction vector

1. INTRODUCTION

Nuclear rector analysis is dependent on the knowledge of the neutron flux. Furthermore, this is given by the solution of the Boltzmann transport equation. This is a seven-dimensional equation (space, time, kinetic energy and solid angle) with no trivial solution.

This equation represents the transport of neutral particles in the absence of electromagnetic fields, i.e. it does not take into account the electrical charge of the particles nor its magnetic moment (spin).

Many deterministic and numerical methods were created in order to solve the transport equation. These methods, e.g. diffusion theory and P_n and S_n methods, result in the reduction of the seven-dimensional phase space and/or in its discretization, what can become a complication when using a thin discretization along all seven dimensions [Sjenitzer, 2013]. Additionally these methods require simplified geometries and specific boundary conditions to achieve solution.

In contrast to these methods is the stochastic Monte Carlo method. This stochastic approach allows the solution of the Boltzmann equation in all seven dimensions and with a continuous phase space. The Monte Carlo method has an error that is proportional to $N^{-1/2}$, in which N is the number of simulated particles and this error is independent of the number of dimensions, whereas numerical methods of the k^{th} order have an error that scales according to $M^{-k/d}$, in which d is the number of dimensions and M the number of discretizations [de Camargo, 2011].

The Monte Carlo simulator used in this work was first developed by Dayana de Carmargo in de Camargo, 2011, and had subsequent advancements in de Camargo et al., 2013, and Barcellos et al., 2015. This program presents a novel procedure in which cross sections are obtained by continuous parametrizations in the range between 0 MeV and 20 MeV, including resolved and unresolved resonances, and with a maximum deviation smaller than 5% from measured data. This procedure allows faster computational time than other models present in the literature (Serpent [Leppänen, 2013], MCNP [Team, 2003], TRIPOLI [Both et al., 2003], OpenMC [Romano and Forget, 2013], KENO [Petrie and Cross, 1975], GEANT [Agostinelli et al., 2003], MCBEND [Cowan et al., 2013]), in which the cross sections are determined from interpolation of cross section data banks.

The developed program computes only down-scattering, due to the severe computational cost of calculating a particle collision without simplifications, and, therefore, neutrons can only have its energy decreased in each scattering reaction. The objective of this work is to prove that up-scattering effects can be implemented without the actual computation of microscopic up-scattering, i.e. the three-dimensional collision of a neutron with an atom or molecule which has a velocity vector that obeys its thermal motion distribution.

This implementation is done by the statistical treatment of the neutron population, which is divided in three distributions. Two of these distributions are the fission distribution, for high neutron energies, and the Maxwell-Boltzmann distribution, for thermal neutron energies. Both distributions have fixed shape, but the population of neutrons in each one can change. The third distribution is an intermediate one, which has, a priori, unknown shape and population, being these two parameters free to vary. The Maxwell-Boltzmann distribution is the one responsible for the inclusion of up-scattering effects, and all distributions are continuous over the whole range of energy present in the simulation.

2. TRANSPORT EQUATION

The *neutron transport equation*, that is also know as *Boltzmann equation*, is the equation that describes the behaviour of the angular neutron flux in a reactor. Being $\phi(\vec{r}, \vec{\Omega}, E, t)$ the angular neutron flux, defined in Equation 2.1 as the angular neutron density times the speed of the neutrons.

$$\phi(\vec{r}, \vec{\Omega}, E, t) \equiv v\, n(\vec{r}, \vec{\Omega}, E, t) \tag{2.1}$$

in which v is the absolute value of the velocity vector of the neutron and $n(\vec{r}, \vec{\Omega}, E, t)$ is the angular neutron density, i.e. the density of neutrons in position $\vec{r}$ that travel in the direction $\vec{\Omega}$ (within the solid angle element $d\vec{\Omega}$) with kinetic energy E (in the range dE) at time t.

It is not the objective of this work to review the whole derivation of the transport equation, this is already very well documented in several sources, such as Duderstadt and Martin, 1979. The most important is the interpretation of the transport equation and the knowledge of the meaning of each of its terms. The Boltzmann equation, as it appears in Sekimoto, 2007, is given by Equation 2.2.

$$\frac{1}{v}\frac{\partial}{\partial t}\phi(\vec{r}, \vec{\Omega}, E, t) + \vec{\Omega} \cdot \nabla\phi(\vec{r}, \vec{\Omega}, E, t) + \Sigma_t(\vec{r}, E, t)\phi(\vec{r}, \vec{\Omega}, E, t) = q(\vec{r}, \vec{\Omega}, E, t) \tag{2.2}$$

in which Σ_t is the total macroscopic cross section and $q(\vec{r}, \vec{\Omega}, E, t)$ represents a neutron source term given by Equation 2.3.

$$q(\vec{r}, \vec{\Omega}, E, t) = \int_0^\infty dE' \int_{4\pi} d\vec{\Omega}' \Sigma(\vec{r}, E' \to E, \vec{\Omega}' \to \vec{\Omega})\phi(\vec{r}, \vec{\Omega}', E', t) + S(\vec{r}, \vec{\Omega}, E, t) \tag{2.3}$$

in which $S(\vec{r}, \vec{\Omega}, E, t)$ is called the external neutron source, i.e. it is a neutron source independent of the angular neutron flux. The term $\Sigma(\vec{r}, E' \to E, \vec{\Omega}' \to \vec{\Omega})$ includes all neutron emission reactions, such as scattering, fission, and $(n, 2n)$ reactions. It can then be rewritten as presented in Equation 2.4.

$$\Sigma(\vec{r}, E' \to E, \vec{\Omega}' \cdot \vec{\Omega}) = \sum_k m_k(E') \Sigma_k(\vec{r}, E') p_k(E' \to E, \vec{\Omega}' \cdot \vec{\Omega}) \tag{2.4}$$

in which $\Sigma(\vec{r}, E' \to E, \vec{\Omega}' \to \vec{\Omega})$ was considered as a function of $\mu_0 \equiv \vec{\Omega}' \cdot \vec{\Omega}$, instead of the two variables $\vec{\Omega}'$ and $\vec{\Omega}$, this is due to cylindrical symmetry along the axis aligned to the incoming particle. Also in Equation 2.4 $m_k(E')$ represents the number of secondary neutrons released by reaction k, e.g 1 for scattering, 2 for $(n, 2n)$ reactions, and ν for fission. $\Sigma_k(\vec{r}, E')$ is the macroscopic cross section of interaction k. Finally the term $p_k(E' \to E, \vec{\Omega}' \cdot \vec{\Omega}) dE d\vec{\Omega}$ represents the probability distribution that reaction k will release a neutron of energy E in the reange dE and direction $\vec{\Omega}$ in the solid angle $d\vec{\Omega}$. In the case of fission $p_f(E' \to E, \vec{\Omega}' \cdot \vec{\Omega})$ is given by Equation 2.5.

$$p_f(E' \to E, \vec{\Omega}' \cdot \vec{\Omega}) = \frac{1}{4\pi} \chi_f(E) \tag{2.5}$$

in which $\chi_f(E)$ is given by Equation 4.10. In the case of scattering $p_s(E' \to E, \vec{\Omega}' \to \vec{\Omega}, A)$ is a bit more complex, since it also depends on the mass number A of the target nucleus, and $\vec{\Omega}'$ is not independent of $\vec{\Omega}$, as will be shown on Chapter 4.

The remaining terms of Equation 2.2 can be labelled as in Equation 2.6, in order to facilitate their description.

$$\underbrace{\frac{1}{v} \frac{\partial}{\partial t} \phi(\vec{r}, \vec{\Omega}, E, t)}_{\text{I}} + \underbrace{\vec{\Omega} \cdot \nabla \phi(\vec{r}, \vec{\Omega}, E, t)}_{\text{II}} + \underbrace{\Sigma_t(\vec{r}, E, t) \phi(\vec{r}, \vec{\Omega}, E, t)}_{\text{III}} = q(\vec{r}, \vec{\Omega}, E, t) \tag{2.6}$$

Term I represents the variation in time of the neutron flux in position $\vec{r}$, direction $\vec{\Omega}$ in the solid angle $d\vec{\Omega}$ and kinetic energy E in the range dE at the instant t. Term II is the net flux between the neutron flux that arrives at point $\vec{r}$ with direction $\vec{\Omega}$ in $d\vec{\Omega}$ and energy E in the range dE at the instant t, and the neutron flux that leaves position $\vec{r}$ with direction $\vec{\Omega}$ in $d\vec{\Omega}$ and energy E in the range dE at time t, when term II is positive the net angular flux is negative. Lastly term III represents the removal of neutrons from the angular flux due to any reaction that comes to pass with the neutron.

It is possible to perceive that the neutron transport equation is, stating in a simple

manner, a neutron balance equation. Nevertheless, the solution of this seven-dimensional equation is far from trivial. It is because of this difficulty that many numerical methods are used. One of these methods is the physical Monte Carlo. This method is chosen because it can easily cope with complex boundary conditions and complex geometries, it can evaluate not only the mean behaviour of a process, but also its moments, and its error decreases by the order of $N^{-1/2}$ (with N the number of samples), being independent of the number of dimensions of the problem.

It is noteworthy that the physical Monte Carlo method is not used to solve directly the transport equation, as opposed to what would happen if a mathematical Monte Carlo method was used, but instead it is used to simulate the microscopic phenomena that occur in a nuclear reactor and which have their representation in the transport equation. Since the results obtained from the stochastic method include the position, direction of travel and kinetic energy of each particle, the neutron flux, the neutron angular flux, among other physical quantities may be obtained from the Monte Carlo results. As a consequence, the solution of the Boltzmann equation can be evaluated.

3. CROSS SECTIONS

The cross section of a nucleus is a measure of the probability a given neutron-nucleus reaction will happen [Glasstone and Sesonske, 1994]. The cross sections depend on the nature of the nucleus, the type of reactions that is considered and the kinetic energy of the reaction measured in the center of mass system.

Should a uniform parallel beam I, in $\frac{neutrons}{m^2\,s}$, of mono-energetic neutrons impinge perpendicularly on a thin plate of differential thickness dx, in m, which has an atomic density of N, in $atoms/m^3$, the rate of reactions per square meter R, in $\frac{reactions}{m^2\,s}$, would be given by Equation 3.1.

$$R = \sigma\, I\, N\, dx \tag{3.1}$$

in which N is the atomic density, shown in Equation 3.2.

$$N = \frac{\rho N_A}{A \times 10^{-3}} \tag{3.2}$$

in which ρ is the density in kg/m^3, N_A is the Avogrado number and it is equal to $6.022 \cdot 10^{23}$ $atoms/moles$, and A is the atomic mass in $g/moles$ (therefore the factor of 10^{-3}). In the case of molecules the same equation can be used, but using the molecular weight M in $g/moles$ instead of A.

It can be noted from Equation 3.1 that σ has an unit of area. As a matter of fact, it is usual to use the unit $[barn]$ to express the cross section, with $1b = 10^{-28}m^2$. The cross section can then be interpreted as the effective area a target nucleus has for a given reaction and with a given collision energy. In this work, if the prefix *microscopic* is omitted the referred cross section is the microscopic cross section, as opposed to the macroscopic cross section, that will be further shown.

Microscopic cross sections for different reactions can be summed, so that the total cross section σ_t is defined as the sum of all possible reactions. Considering only the most relevant reactions for nuclear reactors, the total cross section is given by Equation 3.3.

$$\sigma_t = \sigma_s + \sigma_a \tag{3.3}$$

in which σ_s is the scattering cross section and σ_a is the absorption cross section, which is the sum of the fission cross section σ_f and the radiative capture cross section σ_c.

The product $N\sigma$ is called the macroscopic cross section Σ, in m^{-1}, as shown in Equation 3.4. This can be interpreted as the expected number of interactions a neutron would suffer per unit of travelled length in a given medium (this cannot occur though, for an interaction implies that the neutron is scattered or absorbed).

$$\Sigma = N\sigma \tag{3.4}$$

The inverse of the macroscopic cross section is the mean free path λ, in m, as shown in Equation 3.5. The mean free path is the expected path a neutron will travel in a medium before it interacts with a nucleus.

$$\lambda = \frac{1}{\Sigma} \tag{3.5}$$

For mixtures that contain different nuclear species the macroscopic cross section is given by Equation 3.6. In which n is the number of different atomic or molecular constituents.

$$\Sigma = \sum_{i=1}^{n} N_i \sigma_i \tag{3.6}$$

And the microscopic cross section for a given generic molecule $X_n Y_m$ is given in Equation 3.7.

$$\sigma = n\sigma_X + m\sigma_Y \tag{3.7}$$

Therefore in the case of an homogeneous mixture of two isotopes, e.g. U-235 and U-238, the cross section is given by Equation 3.8.

$$\sigma = \frac{N_{238}\sigma_{238} + N_{235}\sigma_{235}}{N_{238} + N_{235}} \tag{3.8}$$

in which N_{238} and N_{235} are the atomic densities of U-238 and U-235 respectively. For such cases in which two isotopes are present in different weight percentages in a material, their atomic densities can be found by equations 3.9 and 3.10.

$$N_1 = \frac{r\rho N_A}{A_1 \times 10^{-3}} \tag{3.9}$$

$$N_2 = \frac{(1-r)\rho N_A}{A_2 \times 10^{-3}} \tag{3.10}$$

in which r represents the weight percentage of isotope 1. In the case of uranium the weight percentage of U-235 is called enrichment.

4. INTERACTIONS OF NEUTRONS WITH MATTER

Neutrons interact with matter in two ways. Scattering reactions and absorption reactions. Scattering reactions can occur with or without the formation of a compound nucleus, while absorption reactions require the formation of the compound nucleus.

A scattering always results in a neutron leaving the struck atom. An absorption, however, can result in different outcomes, such as the emission of gamma radiation (n, γ), the ejection of an alpha particle (n, ${}_2^4He^{+2}$), the ejection of a proton (n, p), or fission (n, f) [Glasstone and Sesonske, 1994]. Of these, (n, γ) and (n, f) are the noteworthy reactions for thermal reactors.

In all reactions the following quantities must be conserved.*a)* Number of nucleons.*b)* Number of electric charges.*c)* Energy.*d)* Momentum.*e)* Angular momentum.

4.1 Neutron Scattering

Scattering reactions of a neutron with a nuclide are the ones responsible for the slowing down of neutrons in a nuclear reactor, and thus of vital importance for thermal reactors. These interactions can be classified as elastic or inelastic scattering whether the kinetic energy is conserved in a reaction.

Scattering interactions can occur in different manners. The two main ways are the resonance (or compound nucleus) scattering and the potential scattering.

Resonance scattering happens in higher energies in the vicinity of a resonance. In this manner of scattering the neutron and the target nucleus form a compound nucleus and later a neutron is expelled, leaving the nucleus in its ground state (elastic resonance scattering) or in an excited state (inelastic resonance scattering).

Potential scattering can happen in the whole range of energy that a neutron can have in a nuclear reactor [Lamarsh, 1966]. In this form of scattering the neutron is scattered by its interaction with the strong nuclear force of the nucleus and both particles can be treated as in a classical particle collision. The larger part of the slowing down of neutrons in a thermal reactor comes from elastic scattering [Glasstone and Sesonske, 1994].

4.2 Elastic Scattering

Elastic scattering can be determined by considering it a collision of classical particles if both following assumptions can be considered to be true.*a)* The nuclei are at rest relative to the neutron.*b)* The nuclei are not bound in a molecule or a solid [Glasstone and Sesonske, 1994].

These hypothesis are valid for high energy neutrons. According to Sunny et al., 2012, for epithermal neutron energies, i.e. from the order of a few eV to the order of hundreds eV, the free gas model should be used in order to include the thermal motion of the scattering targets. In the thermal range, i.e. up to a few eV, the scattering matrices $S(\alpha, \beta)$ should be used to consider thermal motion and molecule binding effects. Notwithstanding, these models are not used in the present work, for in this contribution the treatment that is given to a neutron depends solely on the distribution to which the neutron belongs. Thus it is considered that neutrons belonging to the fission and intermediate distributions have high enough energies so that the target at rest model can be used, and the neutrons of the thermal distribution have energies that maintain the thermal spectrum, so that for the simplified simulator no interactions have to be calculated explicitly, because the resulting spectrum is preserved and known. More complex models, as the ones previously mentioned, will be considered in future developments of the simulator, but are beyond the scope of the present work.

To find the energy of the neutron after an interaction, it is needed to solve simultaneously the momentum and energy conservation equations, as this are the governing equations for this situation. Although simple, this procedure can become very demanding, in terms of computation, in order to be solved in its most general form. Nonetheless it is possible to apply some simplifications to the problem at hand.

Should the neutron be in the moderating region and have a kinetic energy higher than the thermal region, i.e. of an order greater than eV, then the target nucleus can be considered stationary in relation to the neutron in the laboratory system. This condition already satisfies the prerequisite that the target nuclei are not bound in a molecule or a solid, for the incident neutron energy is large compared to the energy of chemical binding (also of the order of a few eV) and the nuclei can be considered as free. In the further the kinematic procedure for high energy neutrons is sketched.

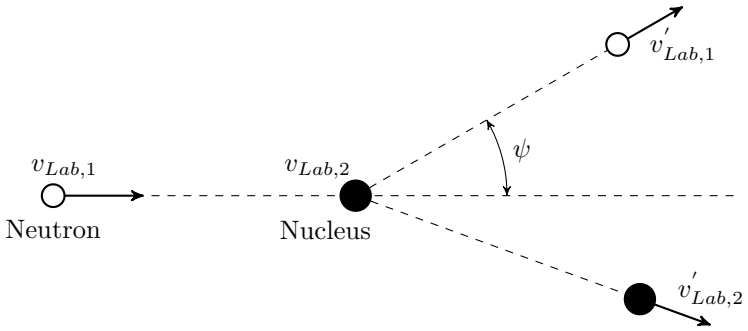

Figure 4.1 – Collision on the laboratory system.

In order to solve the proposed problem, two reference systems are used, the laboratory *Lab* system and the center of mass *CM* system. The laboratory system is the one in which measurements are made, i.e. the energy of the neutron is measured in this system and it is in this system that the nucleus is taken as stationary. The center of mass system is located at the center of mass of both particles (neutron and nucleus) and moves along with it, so that the center of mass remains stationary in this system. The center of mass system provides a simpler treatment of the problem.

In the *Lab* system the neutron has $v_{Lab,1}$ as the magnitude of its velocity vector before the collision and $v'_{Lab,1}$ after it. The nucleus has a speed of $v_{Lab,2} = 0$ prior to the collision and $v'_{Lab,2}$ afterwards. The magnitude of the velocity vector of the center of mass of both particles in the *Lab* system is given by v_{CM} and it is constant, due to conservation of momentum. The *Lab* system is presented in Figure 4.1 and it is easy to perceive that v_{CM} is given by Equation 4.1.

$$v_{CM} = \frac{v_{Lab,1}}{A+1} \tag{4.1}$$

in which A is the mass number of target nucleus.

In the *CM* system the neutron has $v_{CM,1} = v_{Lab,1} - v_{CM}$ as its speed before the collision and $v'_{CM,1}$ after it. The nucleus has a speed of $v_{CM,2} = v_{CM}$ prior to the collision and $v'_{CM,2}$ afterwards. The center of mass of both particles in the *CM* system is stationary. The *Lab* system is presented in Figure 4.2 and it is possible to write $v_{CM,1}$ according to Equation 4.2.

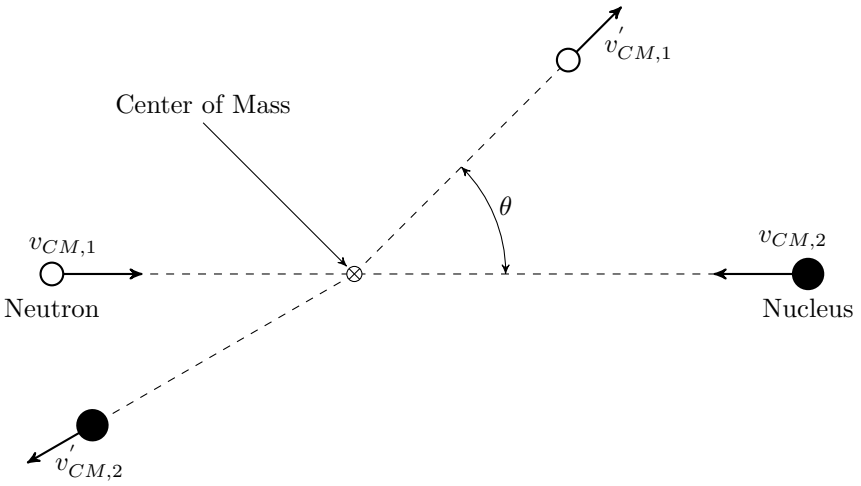

Figure 4.2 – Collision on the center of mass system.

$$v_{CM,1} = \frac{A\, v_{Lab,1}}{A+1} \tag{4.2}$$

From the solution of the equations of conservation of energy and momentum it is possible to arrive at Equation 4.3, as presented in Glasstone and Sesonske, 1994.

$$\frac{E'}{E} = \frac{v'^{2}_{Lab,1}}{v^2_{Lab,1}} = \frac{A^2 + 2\,A\,cos(\theta) + 1}{(A+1)^2} \tag{4.3}$$

in which E is the energy of the neutron in the *Lab* system before the collision, E' is the energy of the neutron in the *Lab* system after the collision and θ is the angle of scattering measured in the *CM* system and that is in the plane that contains both vectors of incident direction and scattered direction of the neutron.

And the relation between the angles θ and ψ are shown in Figure 4.3 and given by Equation 4.4.

$$cos(\psi) = \frac{A\,cos(\theta) + 1}{\sqrt{A^2 + 2\,A\,cos(\theta) + 1}} \tag{4.4}$$

in which ψ is the angle of scattering measured in the *Lab* system and that is in the plane that contains both vectors of incident direction and scattered direction of the neutron.

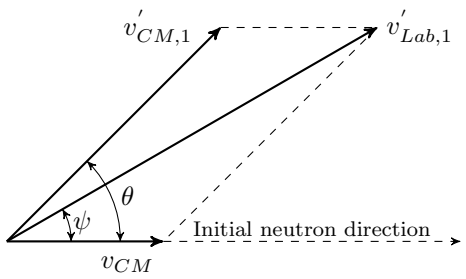

Figure 4.3 – Transformation of angular variables between laboratory and center of mass system.

It is possible to perceive that in Equation 4.3 the neutron can only lose energy and thus only down-scattering is defined. This is in agreement to our hypothesis that the neutron has far greater kinetic energy than the nucleus. Nevertheless it is known that the neutron can gain energy in a scattering reaction if it belongs to the thermal distribution. More specifically, this effect would only be appreciated with neutrons whose kinetic energy is of the same order of magnitude as the thermal energy of the nuclei, i.e. of the order of eV.

As mentioned before, one possible solution of this problem is solving the previous equations of conservation of energy and momentum as before, but this time with a velocity vector for the nucleus in the *Lab* system that is not the null vector. This vector would have a magnitude taken from a thermal distribution and a random direction. This represents a possible solution, but alas is not a practical one since it takes too much processing time. The way this problem is circumvented is shown on the following chapters.

For light nuclei and low collision energies the scattering at the *CM* system is a S-wave scattering, i.e. isotropic. However, as is shown by Lamarsh, 1966, as the target nuclei grow heavier or the collision energies become higher, the differential scattering cross section is no longer constant for all $cos(\theta)$, that means that the scattering is no longer isotropic and other partial wave functions should be taken into account,

When the kinetic energy of a neutron is of the same order of magnitude of the chemical biding energy of the atoms of the molecule involved in the collision (of the order of eV), the nuclide that partakes on the scattering reaction is no longer considered free, but instead it is considered that the molecule, as a whole, participates in the reaction. The

effects of the target nucleus being bound to a molecule are that the scattering cross section becomes higher when compared to other cross sections, and the mass number of the collision target is considered as the entire molecule.

4.3 Inelastic Scattering

Inelastic scattering is a scattering reaction in which the nucleus is left at an excited state after the collision. Therefore, part of the kinetic energy of the particles involved in the interaction is transformed into excitation (internal) energy of the nucleus above its ground state. This energy is later emitted by the nucleus as γ radiation in order to return to its ground state. The γ-ray must be considered in order to solve momentum and energy conservation equations.

Since inelastic scattering leaves the nucleus in an excited state, in order for it to occur, the kinetic energy of participating particles must be, at least, equal to the energy of this first excited state. This represents an energy threshold so that inelastic scattering can be possible. For heavier nuclides this threshold can be quite small, of the order of 44 KeV for U-238, and becomes much higher for lighter atoms, about 6.42 MeV for oxygen, and it does not even occur in hydrogen [Lamarsh, 1966; Glasstone and Sesonske, 1994]. For this reason inelastic scattering is more prominent in heavier nuclei. Exceptions are the magic nuclei, that behave as light nuclei.

Inelastic scattering does, however, occur at low energies (below a few eV). But this does not happen through the formation of a compound nucleus as the aforementioned process, it also does not leave the nucleus in an excited state. This type of inelastic scattering happens when the kinetic energy of the scattered neutron is so low that the target atom is no longer considered as a free atom, but bound in a molecule or in a solid. What takes place is then the interaction of the neutron with the quantum states of vibrational and rotational motion of the molecule (or just vibrational for a solid state). The neutron can then gain or lose energy with such interaction, as a result of a change in these motion states.

The change in the energy of an inelastically scattered neutron by a point-like target is given by Equation 4.5, and the relation between the angles θ and ψ is given by Equation 4.6.

$$\frac{E^{'}}{E} = \frac{v^{'2}_{CM,1}}{v^{2}_{CM,1}} = \frac{\gamma^2 + 2\,\gamma\,cos(\theta) + 1}{(A+1)^2} \tag{4.5}$$

$$cos(\psi) = \frac{\gamma\,cos(\theta) + 1}{\sqrt{\gamma^2 + 2\,\gamma\,cos(\theta) + 1}} \tag{4.6}$$

in which the γ parameter is given by Equation 4.7.

$$\gamma = A\sqrt{1 - \frac{A+1}{A}\frac{Q}{E}} \tag{4.7}$$

In Equation 4.7 Q is the excitation energy of target nucleus [Reuss, 2008]. Should Q be equal to 0, γ is reduced to A.

If neutrons that suffer inelastic scattering have energies that are able to excite only a few energy levels of the nucleus, the outgoing neutrons will have a spectrum that shows distinct energy groups, one for each excitation level. However, if the neutrons have energies that excite the higher and closely spaced energy levels the departing neutrons will present a continuous spectrum, in addition to the discrete one [Lamarsh, 1966].

As presented in Lamarsh, 1966, this spectrum can be defined by Equation 4.8.

$$P(E \rightarrow E^{'}) = \frac{E^{'}}{T^2} e^{\frac{E^{'}}{T}} \tag{4.8}$$

in which T is the nuclear temperature and is given approximately by Equation 4.9.

$$T = 3.2\sqrt{\frac{E}{A}} \tag{4.9}$$

in which T, E and $E^{'}$ are in MeV, A is the mass of target nucleus and the constant 3.2 is in $MeV^{1/2}\,a.m.u.$. It must be remarked that Equation 4.9 is not a very good approximation, specially for magic and near-magic nuclei.

4.4 Fission

In nuclear fission, a heavy nucleus splits into two lighter nuclei and releases energy, since the sum of binding energies of both lighter nuclei is smaller than the binding energy of the original nucleus. Although spontaneous fission can occur in a nuclear reactor, it is a rare event and, therefore, only fission resultant from a neutron absorption will be considered.

For fission to happen an energy threshold for the compound nucleus' must be exceeded. This critical energy can be surpassed just by the binding energy of the last neutron, in which case the nucleus is called fissile and it can be fissioned by neutrons of zero kinetic energy. Should the compound nucleus critical energy be greater than the binding energy added by the absorption of the neutron, the remaining energy must be provided by the kinetic energy of the neutron, in which case the nucleus is called fissionable.

This difference of fissile and fissionable nuclei is shown in the cross sections for these interactions. For fissionable nuclei the cross section is zero up to the difference between the energy threshold and the binding energy of the last nucleon. In the case of fissile nuclei the fission cross section exists for all energies, in fact, it grows towards lower energies according to $1/\sqrt{E}$ and present resonances at higher energies.

Starting with a heavy nucleus, fission results in two lighter nuclei. The atomic number is divided between these fission products, but hardly ever is the number of protons equally divided, i.e. fission is asymmetric. These resulting nuclei are usually in an excited state and will decay in an order of time greater than the time-scale of fission. The distribution of fission products is dependent on both the nuclide that is being fissioned and the neutron energy.

Fission is accompanied by the release of neutrons. The number of neutrons emitted in each fission varies, and the mean depends on both the nuclide and the colliding neutron energy. These neutrons are emitted in two different time-scales, and thus are called prompt and delayed neutrons. Prompt neutrons are the ones emitted in a time-scale of $10^{-14}s$ or less [Glasstone and Sesonske, 1994]. These prompt neutrons represent more than 99% of the neutrons emitted by fission reactions.

The prompt fission spectrum for fission of U-235 is given by Equation 4.10, this is a probability distribution function for the energies of prompt neutrons. Similar data can also be found for other fissionable nuclei, e.g. plutonium.

$$\chi(E) = 0.453\, e^{-1.036\ MeV^{-1}\, E} \sinh \sqrt{2.29\ MeV^{-1}\, E} \tag{4.10}$$

here the energy E is given in units of MeV.

As stated before, fission products can stay in an excited state for a long time before decaying. In their decay chains towards the stability line, these products can decay via neutron emission. The order of time after a fission occurrence these neutrons emitted is of the order of seconds, a time-scale much greater than the time-scale of the prompt neutrons. Delayed neutrons represent less than 1% of neutrons originated by fission, e.g. 0.65% for thermal fission of U-235.

It is common to group delayed neutrons according to their precursors nuclides,i.e. the fission products that will eventually decay and originate a neutron. these precursors have a half-life that can vary from about 55 s to the order of 10^{-1} s. Contrary to prompt neutrons, that have a continuous distribution that spreads along several MeV for their energy, delayed neutrons have much better defined energies that depend on their precursor and are of the order of 10^{-1} MeV.

4.5 Radiative Capture

Radiative capture reactions are one possible outcome of the absorption reaction that captures one neutron in a nucleus, and effectively removes it from the neutron flux. After the formation of a compound nucleus, the increase in the nucleus internal energy due to the neutron binding energy and kinetic energy is evenly divided amongst all nucleons in such a way that the nucleus can stay at this excited state for a long amount of time (in comparison to the time it takes to form a compound nucleus). After some time this excited nucleus decays via emission of gamma-rays.

4.6 Other Interactions

Other interactions of neutrons with nuclides are possible, such as the $(n, 2n)$ and $(n, 3n)$ reactions. These, however, have small cross sections when compared to aforementioned reactions and can be disregarded in a first approach when treating thermal reactors. The

author of this dissertation is aware that, for a full simulation of the reactor core including actinides and fission products these reactions are essential and will be accounted for in a future work, but are neglected in the present stage of the simulator development.

5. PROGRAM DESCRIPTION

As already stated before the C++ Monte Carlo simulator developed in this study distinguishes itself by the usage of functions to obtain microscopic cross-sections that are continuous in energy, in the range from 0 MeV to 20 MeV. This simulator has a similar philosophy to GEANT, in the sense that it performs both tracking and interaction of the particle, what enables a future implementation as a module of this simulation platform. In this chapter, the program structure and the manner in which it proceeds in its calculations will be clarified, and the random number generator will be addressed.

This program can be executed in parallel and the final result is the sum of various executions. In the present case 200 executions were made, each starting with 5000 neutrons, to end up with simulating 10^6 neutron histories. Each execution was allowed to calculate 5000 Monte Carlo steps, but these were also segmented in 50 intervals of 100 steps each, i.e. after 100 steps the simulation reached a checkpoint in which it was halted, the final step data required for its sequence was saved, and then it was restarted using this saved file as the initial condition for the following 100 steps. This procedure was done in order to account for hardware limitations, since increasing the frequency of the save points reduces RAM usage, but it increases the time required for disk writing operations. It also introduces saving tallies regularly during program execution.

5.1 Program Structure

The program simulates each neutron history individually being, therefore, simple to be parallelized. At the beginning of each Monte Carlo step, neutrons created by fission are given two random angles (one between $[0, 2\pi]$ *radians* and the other between $[-\pi/2, \pi/2]$ *radians*) to define their direction and a random energy that obeys the distribution of Equation 4.10, their position is given by the position of the fission reaction the originated them. Other neutrons simply have their energy, position and direction equal as they were at the end of the previous step.

After all the seven parameters that are present in Boltzmann Transport Equation (the ones that are relevant for reactor calculations) are defined, the path that the neutron will travel is selected stochastically, and the position of a reaction is determined. It is also in this

stage that the time interval of the Monte Carlo step is designated. After the displacement of the neutron a check is made to detect an escape, should that be the case the history of the neutron is ended and a new one is selected.

Finally, the type of neutron interaction is selected. This is based on both region and neutron energy, and the process is stochastic, as will be shown in section 5.4. It must be remarked that each steps ends with a reaction. One advantage of this procedure is that there is no position calculation without an interaction, turning the program faster. The downside is that each step has its own time interval and it is established a posteriori.

In the case of a radiative capture the procedure is the same of an escape, the history of the neutron is simply ended, and a new neutron is chosen. In the occurrence of a fission a number of new neutrons is chosen randomly and their are given the position of the reaction. The history of the neutron is then ended, just as the previous cases.

In the general case of scattering (the details will be shown later in this chapter) the energy and the direction angles are updated for the next step. Should the step reach a checkpoint, and hence be the last of an interval of steps, the seven parameters of interest are recorded to be used by the following interval and the history of the neutron is halted.

The main structure of the program is shown on the flowchart of Figure 5.1.

5.2 Geometry and initial condition

The geometry of the reactor is simplified (see Figure 5.2), being described in this program as a $400cm \times 400cm \times 400cm$ cube. The inner part of this cube, Region 1, measures $250cm \times 250cm \times 400cm$ and contains a homogeneous mixture of water and uranium dioxide enriched to 0.73%, and having 25% of its volume as uranium dioxide. Outside this central box there is a square ring, Region 2, that extends to $350cm \times 350cm \times 400cm$ and is composed purely of water. There is a second square ring, Region 3, that is again an homogeneous mixture of water and uranium dioxide, but this one is composed purely of ^{238}U and the dioxide occupies 45% of the volume.

There is a continuity condition on the faces perpendicular to the Z axis at $Z = \pm 200cm$, rendering the reactor infinite along this axis. The program executes the tracking and interaction of neutrons. They are initialised in a random position inside the innermost domain and two angles are randomly chosen from a uniform distribution to define the neutron

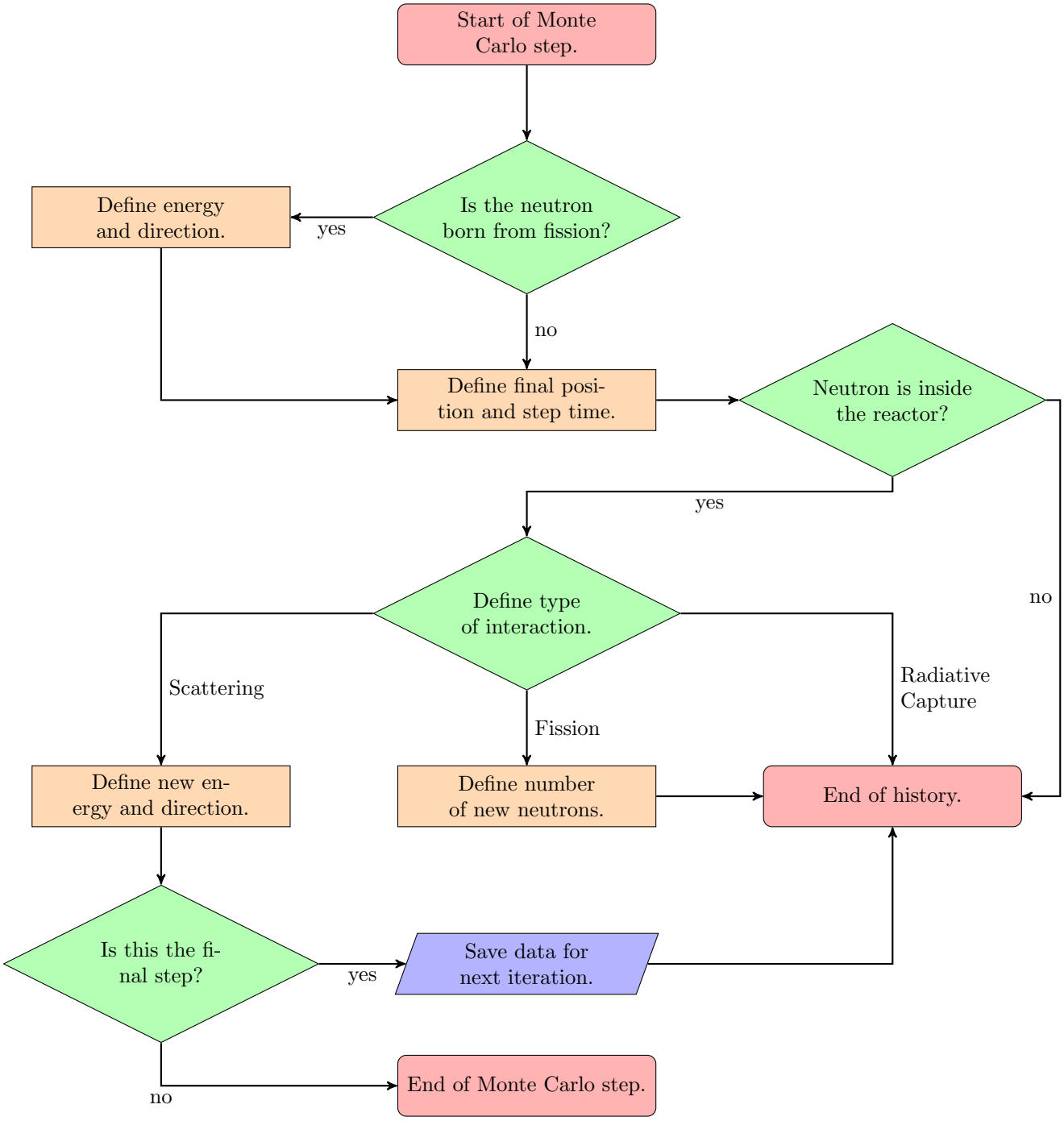

Figure 5.1 – Program simplified flowchart.

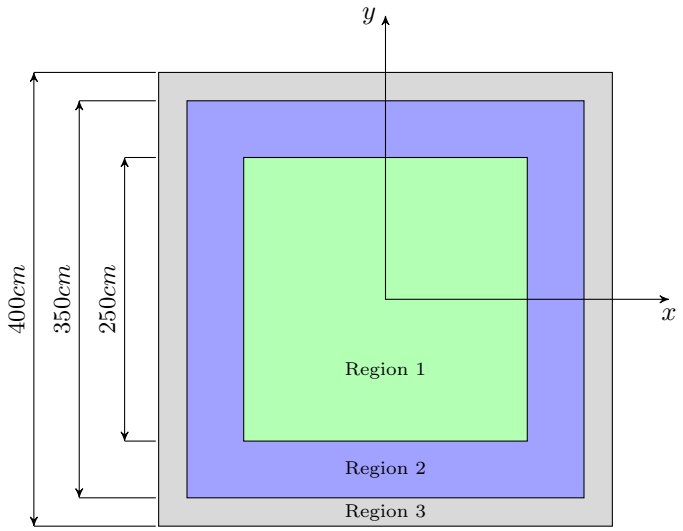

Figure 5.2 – Simulated reactor geometry.

initial path of propagation. One of these angles is chosen from an uniform distribution between $[0, 2\pi]$ *radians* and the other angle is chosen from an uniform distribution between $[-\pi/2, \pi/2]$ *radians*.

5.3 Neutron displacement

To find the position in which a reaction will occur in the end of a Monte Carlo Step it is necessary to know the energy of the neutron, its position at the beginning of the step, the direction of movement and the total macroscopic cross sections for all regions of the reactor. Knowing the initial position and both angles of a spheric system the final position will then be found by the stochastic selection of the length of travelled path.

This decision is done by selecting a multiple S of a mean free path. In order to chose a parameter $S \in [0, \infty)$ a random number $a \in [0, 1)$ is generated and S can be found from Equation 5.1.

$$S = -\ln(1 - a) \tag{5.1}$$

The length of the path is then given by Equation 5.2.

$$L = S\,\frac{1}{\Sigma_t} \tag{5.2}$$

in which Σ_t is the macroscopic cross section for the region in which the neutron is located.

The direction of the neutron is given by the orthonormal vector $\vec{\Omega}$ given by Equation 5.3.

$$\vec{\Omega} = \begin{pmatrix} \cos(\alpha)\,\cos(\beta) \\ \text{sen}\,(\alpha)\,\cos(\beta) \\ \text{sen}\,(\beta) \end{pmatrix} \tag{5.3}$$

in which α is an arbitrary angle between $[0, 2\pi]$ *radians* and β is an arbitrary angle between $[-\pi/2, \pi/2]$ *radians*.

In the case that the neutron crosses a boundary before the path completes the length L, the percentage of S that was actually travelled in the medium is calculated and the remaining portion of S is taken with the total macroscopic cross section of the new region. In fact, this procedure can be repeated for an undetermined number of regions. With this correction L is given by Equation 5.4.

$$L = \sum_i p_i\,S\,\frac{1}{\Sigma_{t,i}} \tag{5.4}$$

in which p_i is the percentage of S that is travelled in the region i with total macroscopic cross section $\Sigma_{t,i}$.

After updating the position of the neutron a test is made to verify that the neutron remains inside the boundaries of the reactor. Should it be outside it is considered that the neutron escaped the reactor, and its history is terminated.

5.4 Choosing the type of interaction

After the position of the interaction is defined, the molecule that is involved in the reaction must be chosen. Should the reaction take place in Region 2 this molecule will be a water molecule, should it be either regions 1 or 3 a random number is generated and

compared to the volume proportions of water and uranium dioxide.

The next step is then to select which type of interaction will come to pass. This is done, once more, by generating a new random number. This number is compared to the ratio of each microscopic cross section of each of the atoms of the molecule by the the sum of all microscopic cross sections (i.e. the total cross section) of all the atoms of the molecule weighted by their stoichiometric proportion and, for the case of enriched uranium, also weighted by the enrichment. For example, the probability of a reaction in uranium dioxide (UO_2) is given by Equation 5.5.

$$p_i = \frac{\sigma_i}{2\,\sigma_{t,O} + e\,\sigma_{t,U-235} + (1-e)\,\sigma_{t,U-238}} \tag{5.5}$$

in which e is the enrichment, $\sigma_{t,O}$ is the total cross section of oxygen-16, $\sigma_{t,U-235}$ is the total cross section of uranium-235, $\sigma_{t,U-238}$ is the total cross section of uranium-238 and σ_i is the cross section of a specific neutron reaction in one of the nuclides of the molecule.

5.5 Fission

If the chosen reaction is a fission two stochastic operations are done. The first one is to decide the number of neutrons born from fission, and the second is to define their energies.

In order to define the number of neutrons born from fission a random number is generated between 0 and 0.972, should this number be $\leqslant 0.5$ two new neutrons are created, should it be > 0.5 then 3 new neutrons are generated. This procedure has as its average 2.48 neutrons born per fission, which is the mean for fissions induced by thermal neutrons. It is clear that this simplified treatment does not take into account the shift that happen in this mean when the energy of the neutrons increases, this is considered a good approximation since, in thermal reactors, most fissions occur due to thermal neutrons. It is also not possible to have numbers different from 2 or 3 new neutrons being, the rarer cases in which more, or less, neutrons are generated are neglected. It must be stated that all neutrons are considered prompt neutrons, and this reactor has no delayed neutrons.

The energy of the neutrons born from fission come from the energy distribution for prompt neutrons given by Equation 4.10. All neutrons created by fission are given a prompt neutron energy. The position of the fission reaction is also recorded for it is the

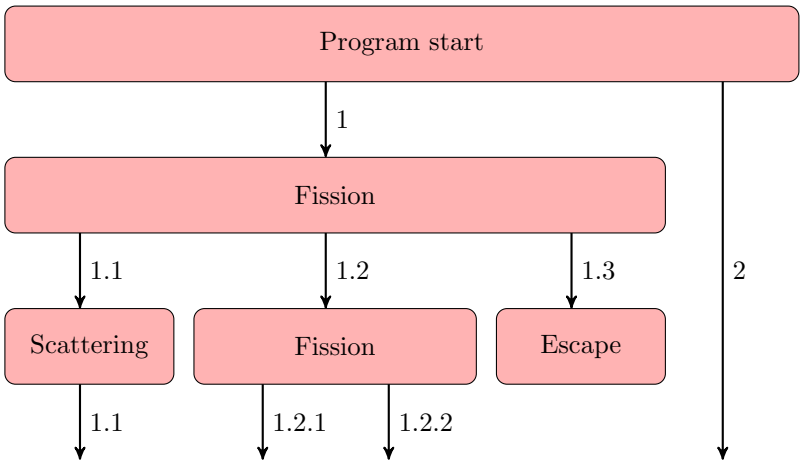

Figure 5.3 – Order of neutron histories.

initial position of the next Monte Carlo step of the newly generated neutrons.

In the circumstance of a fission the histories of the neutrons produced by fission are computed before the ones of other neutrons, and this procedure is done on the opposite order the neutrons are produced, i.e. the history of the last generated neutron is the next to be computed. In order to clarify this procedure Figure 5.3 contains a flowchart of possible outcome.

In Figure 5.3 neutrons 1 and 2 are neutrons from the starting population. The first neutron to have its history computed is neutron 1. This neutron then takes part in a fission reaction that generates 3 new neutrons. The next history to be computed is then the one of neutron 1.1 and then, after this history ends, the one of neutron 1.2. In this case neutron 1.2 also partakes in a fission, the history of the neutrons created in this fission, neutrons 1.2.1 and 1.2.2 take precedence over the history of neutron 1.3. All these histories come before the one of neutron 2 that is, as was neutron 1, a neutron from the starting population.

5.6 Scattering

In the case the chosen reaction is a scattering reaction, a new energy and a new direction must be given to the neutron. A simplification of the program is that is considers the scattering as isotropic in the center of mass system. As seen on previous chapters the scattering is isotropic for low kinetic energies and small nuclei, and, as the collision energies become higher and/or target nuclei become larger, anisotropy becomes distinguishable.

In order to find the new energy of the neuron a random number θ is generated between 0 and π, and Equation 4.3 is used. Again, this equation only accounts for down-scattering.

It is necessary to implement up-scattering effects in the program. This is done via the statistical treatment of the neutron population. To achieve this objective after each scattering a test is made to define whether a neutron belongs to the thermal equilibrium population or not.

This test is performed by the generation of a random number between 0 and 1 and by the comparison of this number with the Maxwell-Boltzmann cumulative distribution for the hypothetical thermal equilibrium temperature of 568 K. Should the random number be grater than the cumulative distribution, then the neutron is considered to be in thermal equilibrium with the moderator. Neutrons that are part of the thermal population are assigned a new energy, sampled from the Maxwell-Boltzmann probability distribution. This new energy is then kept constant, regardless of the number of collisions the neutron suffers, this is done so that the thermal spectrum is maintained. It is also after the first scattering that the neutron is no longer considered as part of the fission population. It must be remarked that this test is realized after each scattering a neutron that is not part of the thermal distribution suffers, and, as a consequence of the continuum energy consideration, there are no energetic thresholds for its occurrence, so that the distributions have superimposed regions.

According to Bell and Glasstone, 1970, for large well-moderated reactors with homogeneous temperature, the Maxwell-Boltzmann distribution can be a good approximation for the thermal neutron spectrum. This, however, is not the case for heterogeneous reactors with large temperature gradients, in which a more detailed treatment is required.

The procedure to find the new neutron direction after the scattering collision are a bit more complex, due to the three-dimensional nature of the problem. The change in angle from the direction the neutron was travelling before the interaction is given by Equation 4.4. This angle, however, is measured on the plane that contains both before and after scattering directions. In the full three-dimensional problem this plane can be any plane that contains the initial direction of travel of the neutron.

In order to solve this problem we must find two auxiliary normal vectors $\vec{\Omega}_P$ and $\vec{\Omega}_Q$

that are orthogonal between themselves and the initial direction vector $\vec{\Omega}_i$, which is given by Equation 5.6. To find these two auxiliary vectors, an arbitrary final direction vector $\vec{\Omega}_f^*$ that is on the vertical plane is used. The equation for $\vec{\Omega}_f^*$ is given in Equation 5.7. It must be noted that both vectors are unitary.

$$\vec{\Omega}_i = \begin{pmatrix} \cos(\alpha)\ \cos(\beta) \\ \text{sen}\,(\alpha)\ \cos(\beta) \\ \text{sen}\,(\beta) \end{pmatrix} \tag{5.6}$$

$$\vec{\Omega}_f^* = \begin{pmatrix} \cos(\alpha)\ \cos(\beta+\psi) \\ \text{sen}\,(\alpha)\ \cos(\beta+\psi) \\ \text{sen}\,(\beta+\psi) \end{pmatrix} \tag{5.7}$$

in which α is an arbitrary angle between $[0, 2\pi] radians$, β is an arbitrary angle between $[-\pi/2, \pi/2] radians$ and ψ is an angle between $[0, \pi] radians$ given by the solution of Equation 4.4.

Since the vectors $\vec{\Omega}_P$ and $\vec{\Omega}_Q$ are orthogonal and unitary, the vectors resulting from their sum and from their subtractions are also orthogonal between themselves. Using this and the fact that $\vec{P}$ and $\vec{Q}$ can point in any given direction, they can be found by solving the system in Equation 5.8.

$$\begin{cases} \dfrac{\text{sen}\,(\psi)}{\sqrt{2}}\,(\vec{\Omega}_P - \vec{\Omega}_Q) = \vec{\Omega}_i \times \vec{\Omega}_f^* \\ \dfrac{\text{sen}\,(\psi)}{\sqrt{2}}\,(\vec{\Omega}_P + \vec{\Omega}_Q) = \vec{\Omega}_f^* - \cos(\psi)\,\vec{\Omega}_i \end{cases} \tag{5.8}$$

in which $\sqrt{2}$ is responsible for the normalisation of the vectors.

By solving the system of Equation 5.8 $\vec{\Omega}_P$ and $\vec{\Omega}_Q$ can be found. Then they can be used on the rotation of the arbitrary vector of the final direction $\vec{\Omega}_f^*$ around the vector of initial direction $\vec{\Omega}_i$. therefore, the final direction of the neutrons after the collision $\vec{\Omega}_f$ is given by Equation 5.9.

$$\vec{\Omega}_f = \cos(\psi)\,\vec{\Omega}_i + \text{ sen}\,(\psi)\,(\cos(\Phi)\,\vec{\Omega}_P \pm \sqrt{1-\cos(\Phi)^2}\,\vec{\Omega}_Q) \tag{5.9}$$

which can be simplified as

$$\vec{\Omega}_f = \cos(\psi)\,\vec{\Omega}_i + \text{ sen}\,(\psi)\,(\cos(\Phi)\,\vec{\Omega}_P + \text{ sen}\,(\Phi)\,\vec{\Omega}_Q) \tag{5.10}$$

in which Φ is a random angle between 0 *radian* and 2π *radians*.

As a closure it must be stated that the scattering reaction differs between neutrons above 1 eV and below this threshold. The difference is that for neutrons above 1 eV the scattering considers the atom as a free atom, and only the mass of the nuclide is considered. For neutrons below 1 eV the atoms are considered bound in the molecules, and the mass of all the nuclides of the molecule are considered.

5.7 Sampling from the Maxwell-Boltzmann Distribution

In order to sample energies from the Maxwell-Boltzmann distribution, the cumulative distribution function was inverted numerically. This was done by sampling the cumulative distribution function in 10001 equally spaced points in the range 0 eV to 1 eV, inverting the coordinates of these points and performing linear interpolation in all 10^4 intervals.

The value of the integral of the Maxwell-Boltzmann probability distribution function, for the temperature of 568 K, between the limits 1 eV and $+\infty$ is smaller than 10^{-8}, and the integral between 0 eV and 1 eV can be approximated to the unit.

This procedure was tested with 10^5 random values between 0 and 1. The normalized histogram of the attained energy values is shown in Figure 5.4 with the Maxwell-Boltzmann probability distribution function superimposed.

5.8 Random Number Generator

Monte Carlo simulations require a great number of random numbers. Therefore, it is needed that the random number generator used be uniformly distributed and have a long period. The default random generator of C library *stdlib.h* is, therefore, not suitable, since

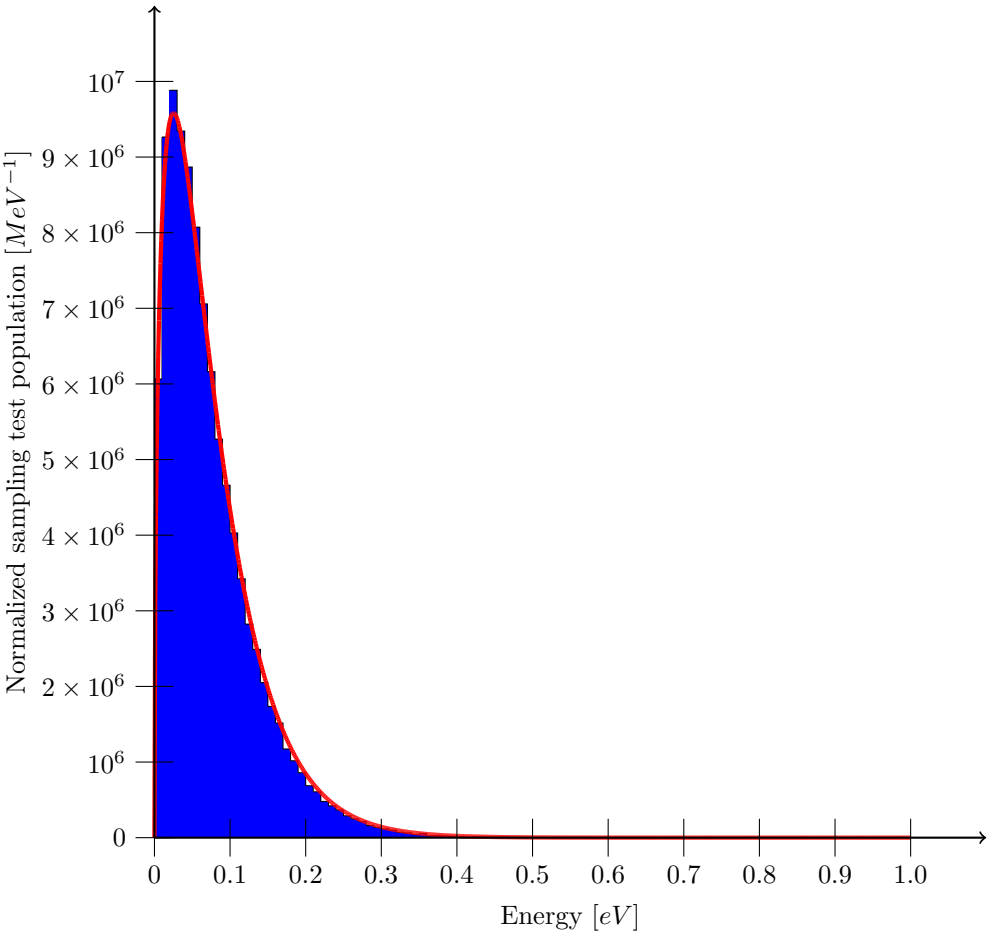

Figure 5.4 – Sampled Maxwell-Boltzmann population.

its period is of just 32767 values.

For this reason the random number generator that was used was Mersene Twister, a pseudorandom number generating algorithm developped by Makoto Matsumoto and Takuji Nishimura that has a proven period of $2^{19937} - 1$ values, and has a speed very similar to the *rand()* function. This random number generator has passed Marsaglia diehard test [Marsaglia, 1985]. The 64-bit version of the program was used and three functions were employed according to the simulated stochastic process, one that generated real numbers in the $[0, 1]$ interval, one that generated real number in the $[0, 1)$ interval, and the last that generated real numbers in the $(0, 1)$ interval.

For a better understanding of Mersenne Twister random number generator it is recommended the reading of the article Matsumoto and Nishimura, 1998, in which the generator is proposed. The software can be downloaded freely at *http://www.math.sci.hiroshima-u.ac.jp/ m-mat/MT/emt.html*, where an extended bibliography on the subject can also be found.

In the Appendix section Mersenne Twister copyright the disclaimer can be found.

6. RESULTS

Results were obtained for a starting population of 10^6 neutron histories. The Monte Carlo simulation was performed for 5000 Monte Carlo steps, organized in 50 intervals of 100 steps each. The total of 10^6 initial particles was attained by 200 consecutive executions of the simulation, each with a starting population of 5000 neutrons. The whole process of simulation was automated by the scheduling of the executions.

The behaviour of the total population along all 5000 Monte Carlo steps is shown on Figure 6.1. Since the initial calue of the vertical axis of this graphic is 5×10^5 to provide a better visualisation, a detail is added to allow a better comprehension of the scale.

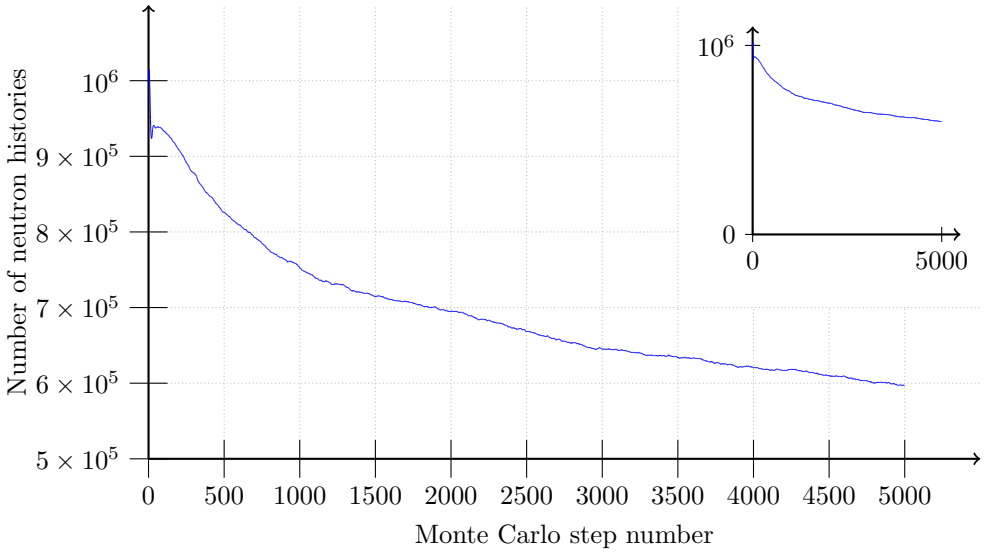

Figure 6.1 – Total of neutron histories.

By inspection of Figure 6.1 it is clear that the simulated reactor is sub-critical, this will be supported by the computation of the neutron multiplication factor, which will be shown further. It is also possible to note an increase of the number of neutrons along the first steps of the simulation. This behaviour, in opposition to the sub-critical tendency, is attributed to the fact that the simulation is started with a purely fission distribution.

The total population is taken as the sum of three distributions, the thermal, the intermediate and the fission one, each with its own time dependent population. Each of these populations are presented in figures 6.2 to 6.4. Note that the vertical axis of the

graphics in Figure 6.3 does not have its origin at zero.

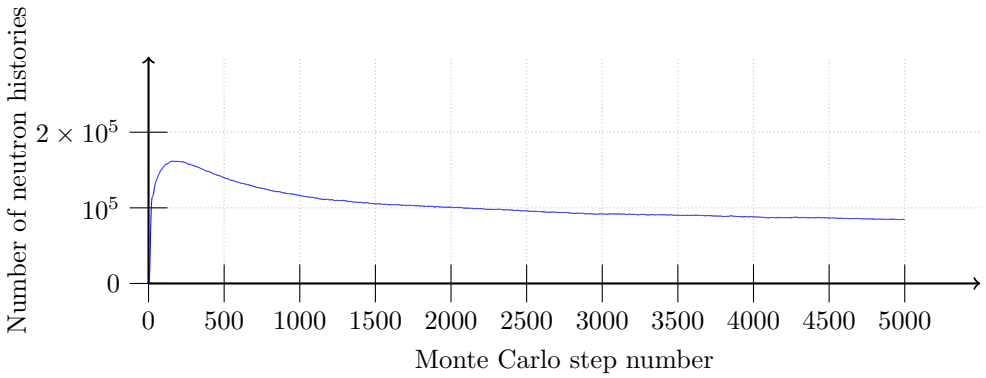

Figure 6.2 – Thermal distribution population.

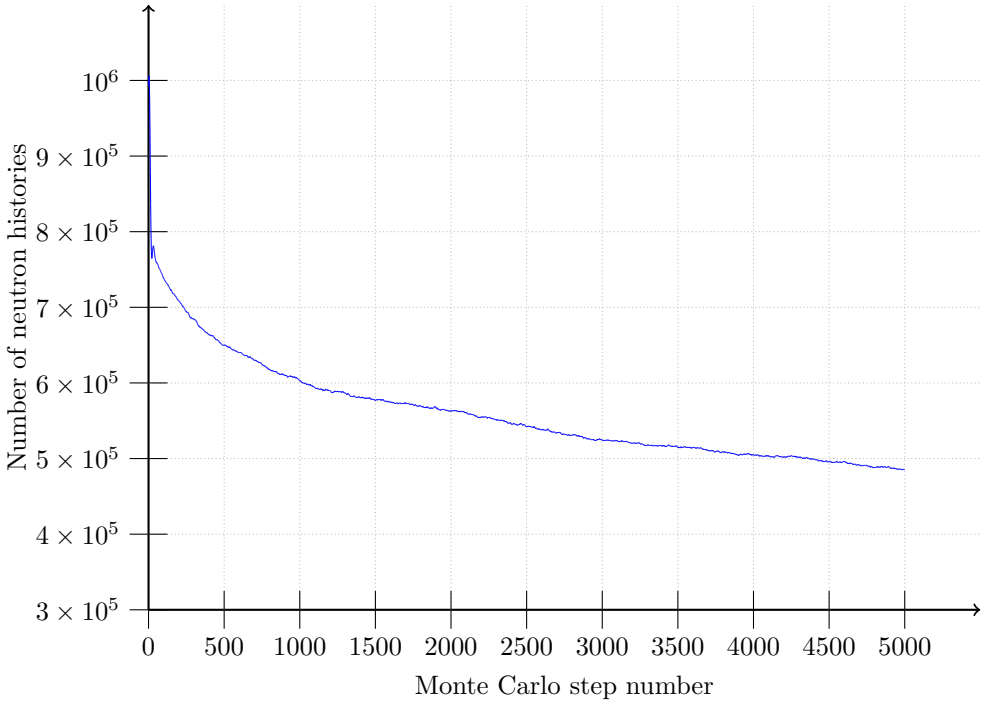

Figure 6.3 – Intermediate distribution population.

In figures 6.5 to 6.7 the ratios of the populations of each of the distributions in each step by the total population in each step are shown. Note that the vertical axis of the graphic in Figure 6.6 does not have its origin at zero.

In figures 6.5 to 6.7 it is perceivable that, even though the total population varies, the proportion between each distribution is relatively constant. This, of course, after the bias of the initial population is no longer recognizable. This maintenance of these ratios is

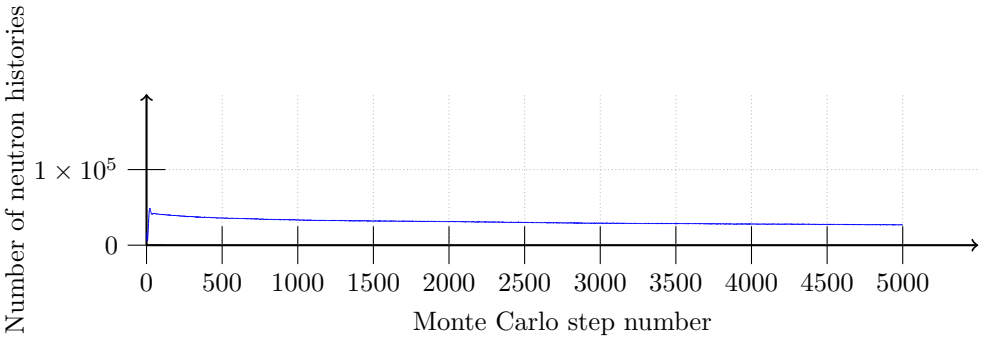

Figure 6.4 – Fission distribution population.

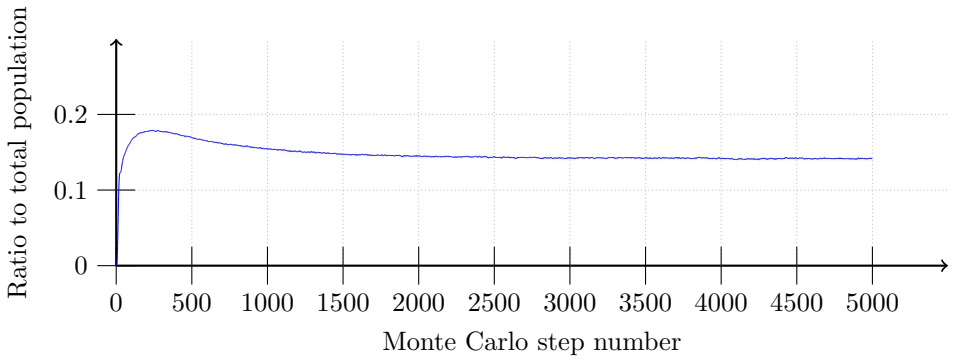

Figure 6.5 – Thermal distribution ratio.

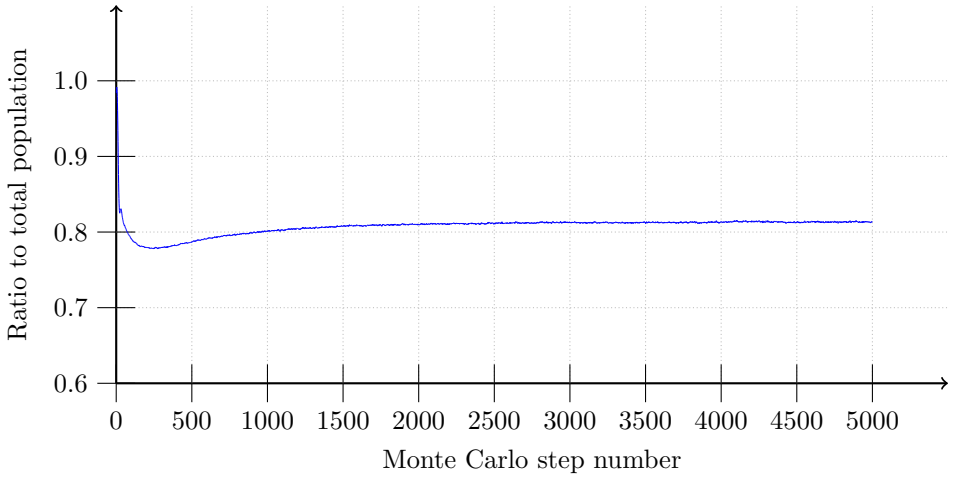

Figure 6.6 – Intermediate distribution ratio.

fruit of the fact that the neutron spectrum is constant along the Monte Carlo steps.

It is possible to compute the first moment M_1 of the data presented in the graphics of figures 6.5 to 6.7, as well as the second M_2, third M_3 and fourth M_4 moments about the

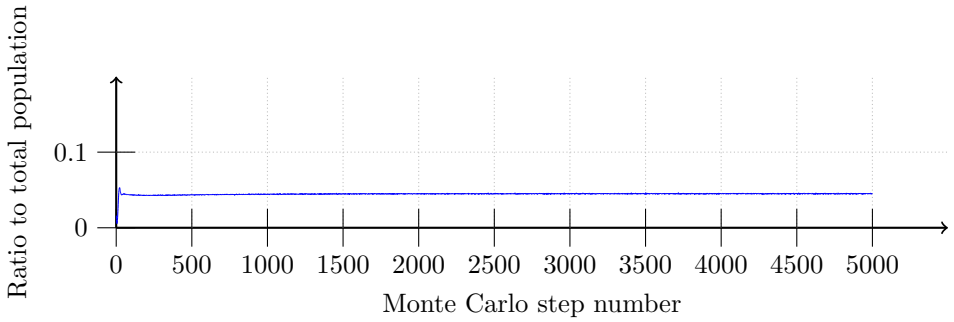

Figure 6.7 – Fission distribution ratio.

mean. These moments are presented on tables 6.1 to 6.3. This moments act as an indicative that the simulated population has enough elements, so that the statistical fluctuations are small. It is important to define the statistical fluctuations, to the end of, if future works, use the simulation results together with deterministic models.

Table 6.1 – Statistical moments of the proportion of the thermal population.

M_1	M_2	M_3	M_4
1.47704×10^{-1}	1.51347×10^{-4}	-4.72400×10^{-6}	9.32240×10^{-7}

Table 6.2 – Statistical moments of the proportion of the intermediate population.

M_1	M_2	M_3	M_4
8.07475×10^{-1}	2.90160×10^{-4}	-9.54065×10^{-5}	8.69776×10^{-5}

Table 6.3 – Statistical moments of the proportion of the fission population.

M_1	M_2	M_3	M_4
4.48216×10^{-2}	1.85783×10^{-4}	1.74201×10^{-4}	1.66486×10^{-4}

On tables 6.1 and 6.2 is possible to observe that the second, third and fourth moments about the mean are several orders of magnitude smaller that the mean, thus indicating small statistical fluctuations. Also, since the third moment is small when compared to the mean, the asymmetry of the data about the mean can be neglected. On Table 6.3 the second, third and fourth moments have the same order of magnitude, which are two orders of magnitude smaller then the mean, this happens due to the fact the the fission population

is the smallest among the three distributions (excluding the first few steps) and a larger population should be simulated to attain a better statistical representation of the fission population.

The mean time length of each Monte Carlo step for the total population is presented in Figure 6.8, and in figures 6.9, 6.10 and 6.11 the mean Monte Carlo time interval for neutrons belonging to the thermal, intermediate and fission distributions respectively.

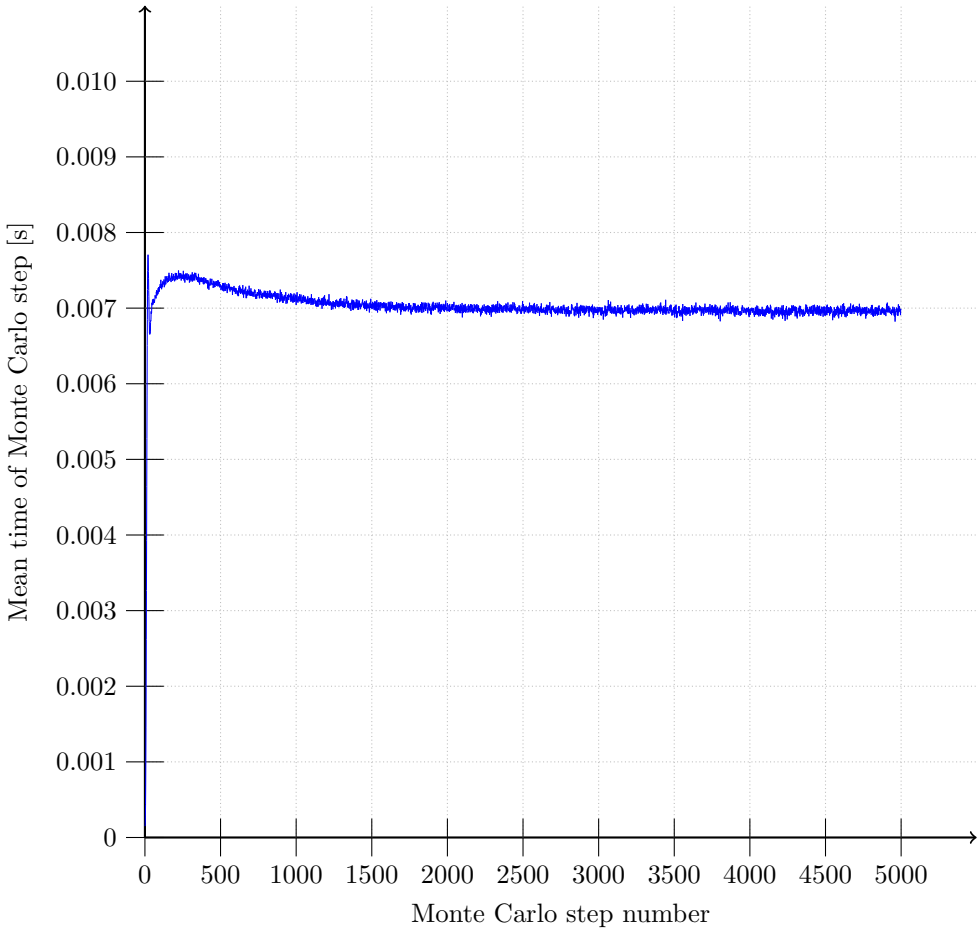

Figure 6.8 – Equivalence of Monte Carlo step and mean time interval.

Again, the first moment as well as the second, third, and fourth moments about the mean of the data presented in figures 6.8 to 6.11 are calculated. The moments of each data set are presented in tables 6.4 to 6.7, respectively.

It is possible to perceive on tables 6.4 to 6.7 that the second moment is already several orders of magnitude smaller than the mean, and the third and fourth moments are negligible compared to it. This indicates that, not only the data has a small spread about

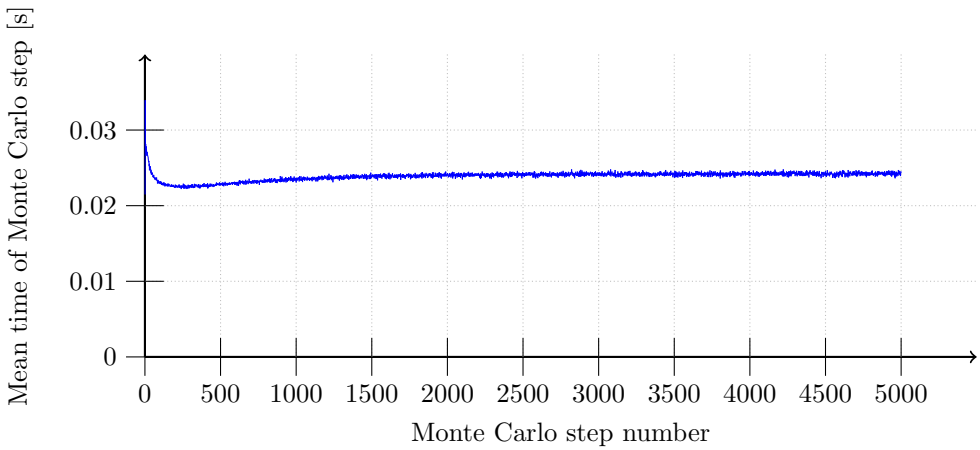

Figure 6.9 – Equivalence of thermal distribution Monte Carlo step and mean time interval.

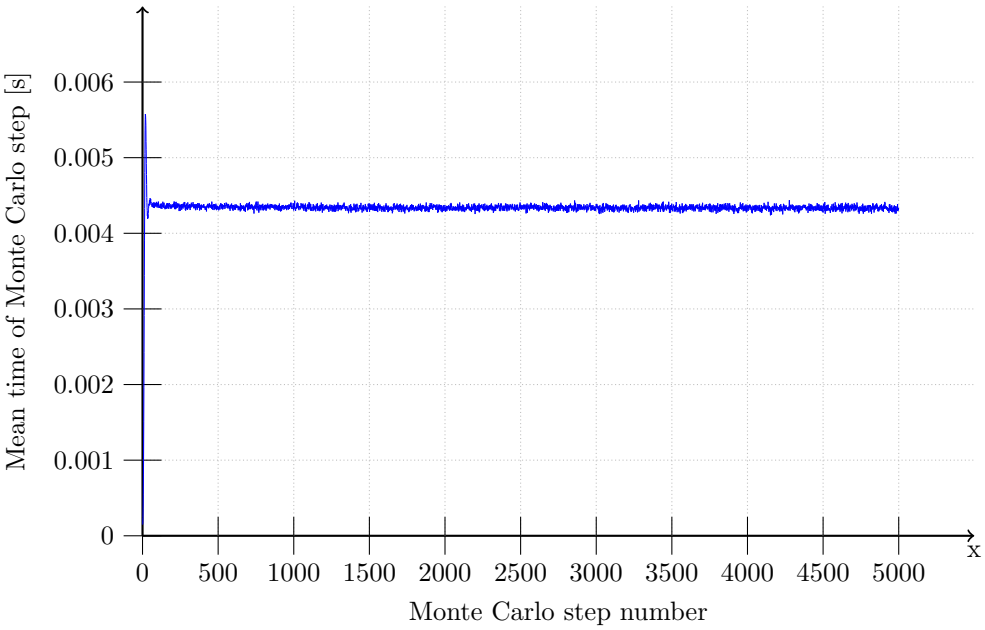

Figure 6.10 – Equivalence of intermediate distribution Monte Carlo step and mean time interval.

Table 6.4 – Statistical moments of the mean step time interval determination of the total population.

M_1 $[s]$	M_2 $[s^2]$	M_3 $[s^3]$	M_4 $[s^4]$
7.02778×10^{-3}	1.00283×10^{-7}	-5.01673×10^{-10}	3.17902×10^{-12}

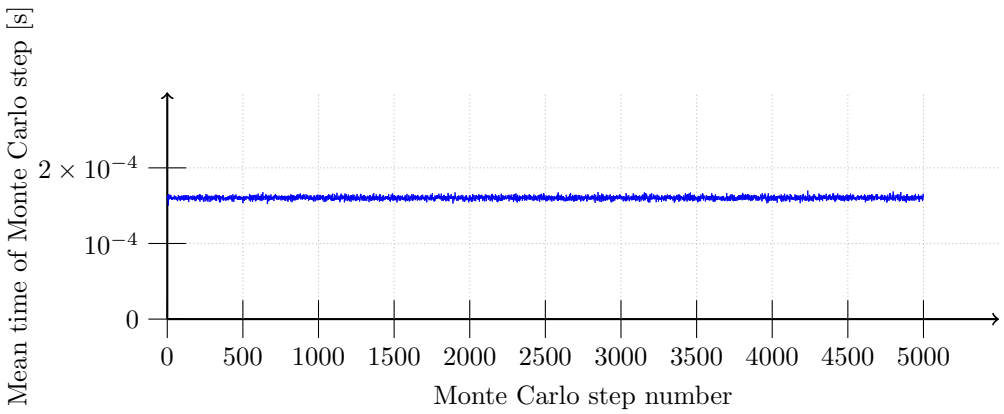

Figure 6.11 – Equivalence of fission distribution Monte Carlo step and mean time interval.

Table 6.5 – Statistical moments of the mean step time interval determination of the thermal population.

M_1 $[s]$	M_2 $[s^2]$	M_3 $[s^3]$	M_4 $[s^4]$
2.38849×10^{-2}	3.34920×10^{-7}	1.65753×10^{-10}	2.83049×10^{-12}

Table 6.6 – Statistical moments of the mean step time interval determination of the intermediate population.

M_1 $[s]$	M_2 $[s^2]$	M_3 $[s^3]$	M_4 $[s^4]$
4.33481×10^{-3}	2.79730×10^{-8}	-8.87868×10^{-11}	3.46510×10^{-13}

Table 6.7 – Statistical moments of the mean step time interval determination of the fission population.

M_1 $[s]$	M_2 $[s^2]$	M_3 $[s^3]$	M_4 $[s^4]$
1.60344×10^{-4}	5.23663×10^{-12}	3.12344×10^{-19}	8.38639×10^{-23}

its mean, but also the fluctuations can be taken as symmetric.

One important information that can be attained from the simulation is the effective neutron multiplication factor. This can be evaluated by dividing the number of fissions caused by neutrons of one generation by the number of fissions caused by neutrons of the previous generation, in such a way that each time neutrons are created by fission they belong to a generation that follows the generation of the neutron that induced the fission reaction.

Along the 5000 Monte Carlo step 252 neutron generation were identified. The neutron multiplication factor from one generation to the next is presented in Figure 6.12.

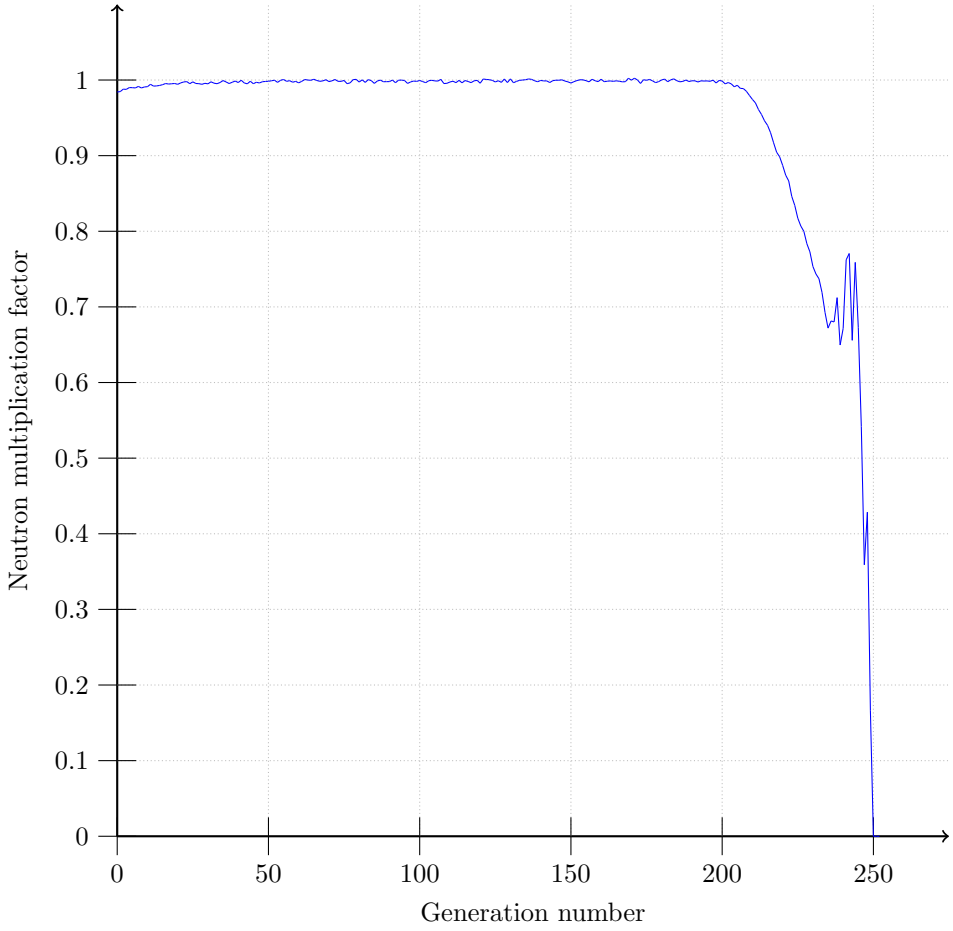

Figure 6.12 – Multiplication factor from the neutron life cycle.

In Figure 6.12 it is possible to note that, after generation number 200, the neutron multiplication factor deviates from the behaviour presented in previous steps. This can be explained by the fact that neutrons of different generations are present in a same Monte Carlo step and, as the simulation come to its end on step 5000, the number of neutrons in a generation that causes fission diminishes for the later generations, which is an artefact due to the way this simulation is terminated. The first generations are also less representative, for they are still in the transient region.

The geometric mean of the neutron multiplication factor was calculated, to this end generations 20 to 200 were taken into account. This resulted in an effective neutron multiplication factor of 0.998417.

The mean number of Monte Carlo steps of generations 20 to 200 was also computed, as well as its second, third and fourth moments about the mean. This data is presented in Table 6.8.

Table 6.8 – Statistical moments of the neutron life cycle related Monte Carlo step numbers.

M_1	M_2	M_3	M_4
2.29305×10^{1}	2.18853×10^{-3}	8.96524×10^{-5}	1.75426×10^{-5}

On Table 6.8 it is possible to note that the the moments about the mean are several orders of magnitude smaller that the mean, what indicates small statistical fluctuations. Also, by comparing the order of magnitude of the third moment about the mean with the order of magnitude of the other moments, it is possible to infer that the asymmetry about the mean is negligible. Consequently the simulated results can be considered significant.

Another result obtained from the simulation is the representation of the neutron spectrum of each distribution (and subsequently of the total population) for each step. The spectra are presented as histograms, even tough the energy is computed continuously, to the end of reducing the size of the data output of the simulation. Also, due to the fact that the neutron energies encompass several orders of magnitude, from 0 eV to 20 MeV, the histograms are evaluated in three energy ranges. The first is between 0 eV and 1 eV and it is divided in 100 bins of equal energy range. The second energy extent is between 1 eV and 0.1 MeV and it is divided in 500 bins whose energy range grows exponentially. The final interval is between 0.1 MeV and 20 MeV, and it is divided in 100 bins of equal range.

In each energy interval the histograms are normalized, in order to render the comparison between spectra independent of the population at a respective Monte Carlo step. In the presented results each histogram is normalized taking into account only the population inside the displayed energy interval.

The step that was chosen to portray the spectrum was step number 2000, which has a population of 695074 neutrons, being 100957 thermal neutrons, 562815 part of the intermediate distribution and 31302 of the fission distribution. This step was chosen because it is in the region where the ratios between distributions is in a pseudo-permanent state and it has a high number of neutrons, being, therefore, a good candidate to depict the permanent neutron spectrum.

The spectrum of the total population of step 2000 is shown in figures 6.13, 6.14 and 6.15.

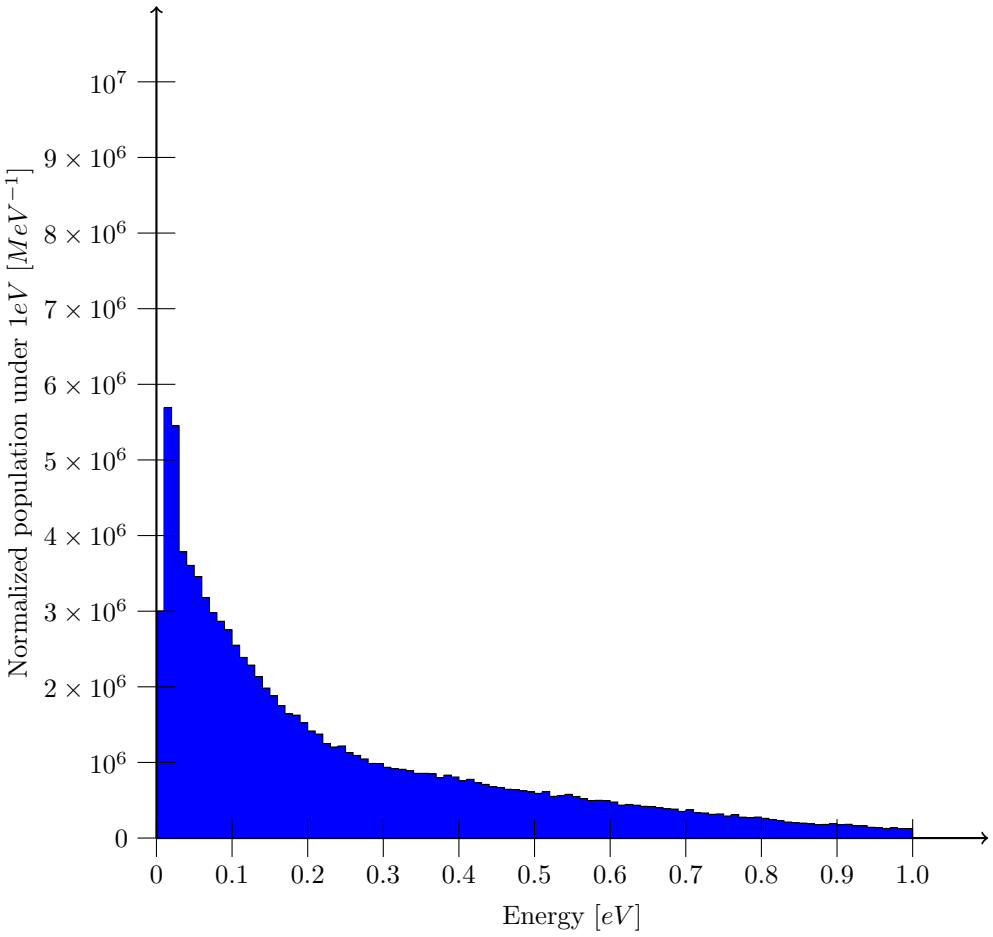

Figure 6.13 – Total population spectrum in the first energy interval for step 2000.

The thermal population is all contained within the first energy extent, between 0 eV and 1 eV. This is shown for step 2000 in Figure 6.16 with the Maxwell-Boltzmann distribution for the temperature of 568 K for comparison.

The spectrum of the intermediate population of step number 2000 is shown in figures 6.17, 6.18 and 6.19.

Finally the fission spectrum of step 2000 is shown in figures 6.20 and 6.21 with the prompt fission distribution given by 4.10. In Figure 6.20 the histogram, after being normalized, is multiplied by 0.013, since this is the numerical result of the integral presented in Equation 6.1. And in Figure 6.21 the histogram is multiplied by 0.987 after its normalization, for this is the approximately numerical result of the integral of Equation 6.2.

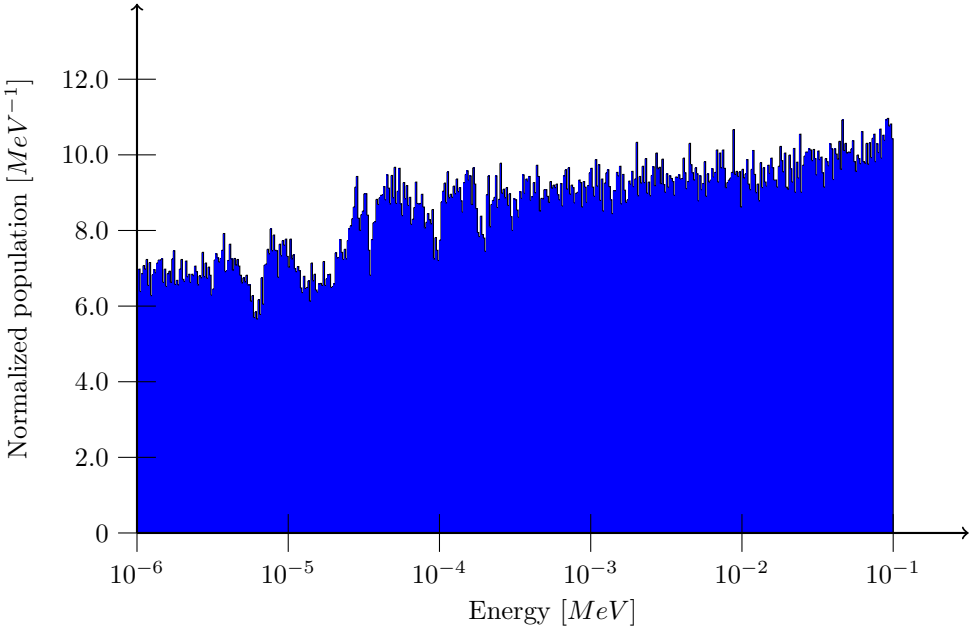

Figure 6.14 – Total population spectrum in the second energy interval for step 2000.

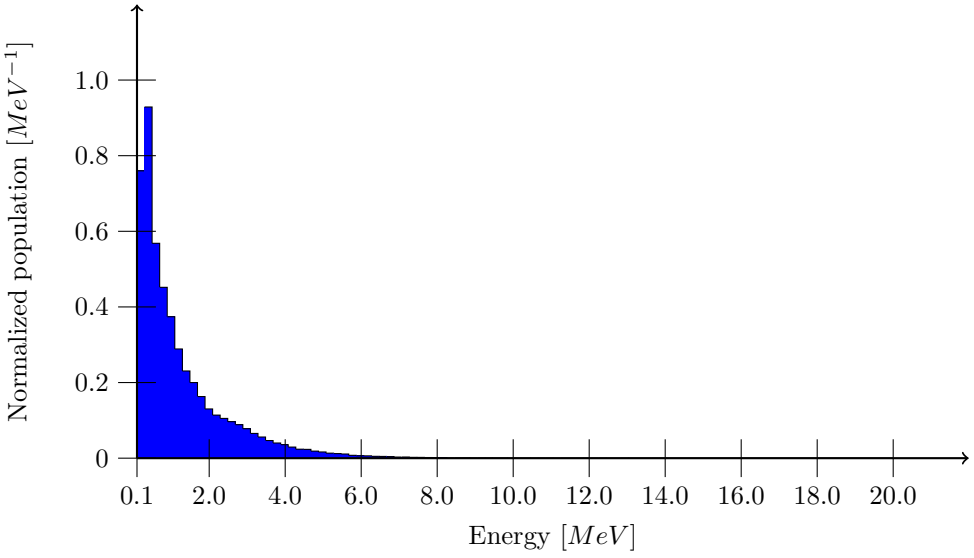

Figure 6.15 – Total population spectrum in the third energy interval for step 2000.

$$\int_0^{0.1MeV} 0.453\, e^{-1.036\ MeV^{-1}\,E} \sinh\sqrt{2.29\ MeV^{-1}\,E}\ dE \tag{6.1}$$

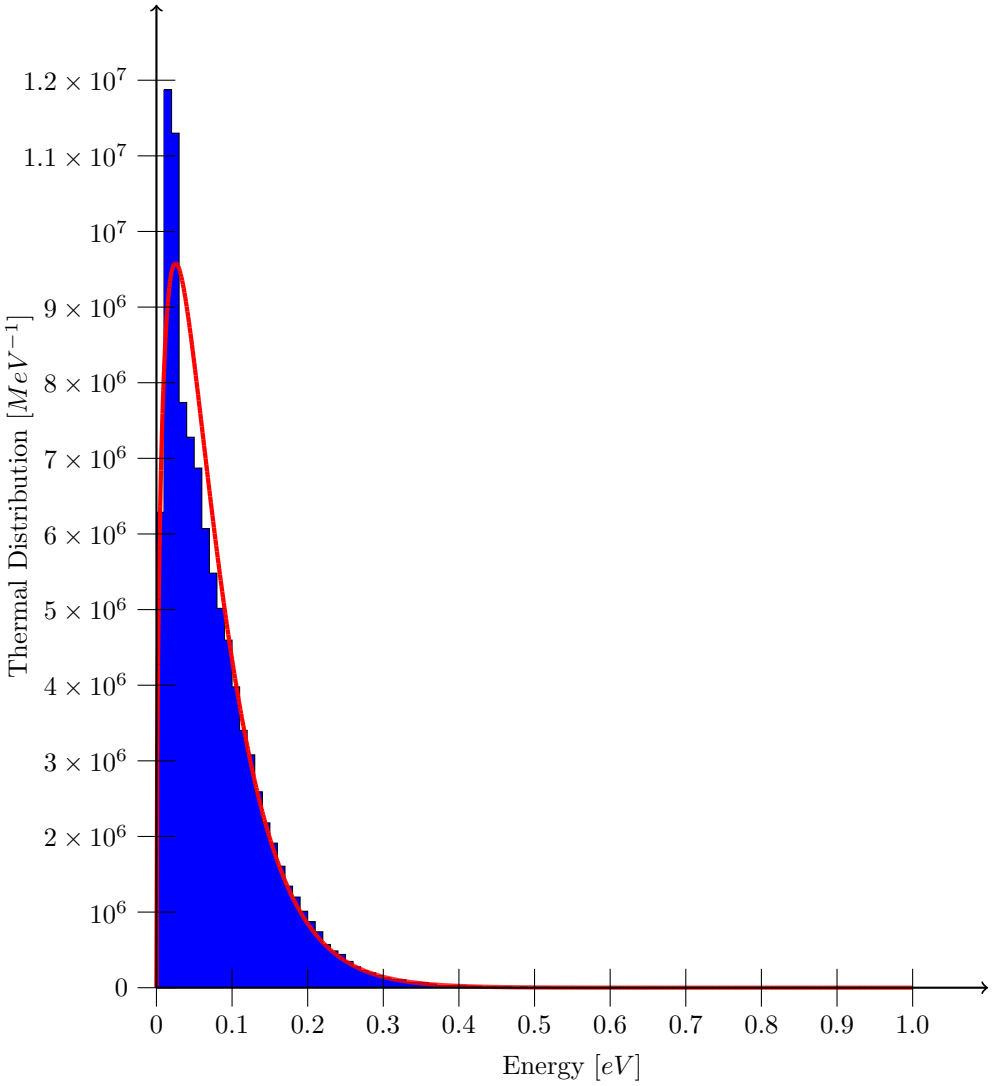

Figure 6.16 – Thermal population spectrum in the first energy interval for step 2000.

$$\int_{0.1MeV}^{20MeV} 0.453\, e^{-1.036\ MeV^{-1}\,E} \sinh\sqrt{2.29\ MeV^{-1}\,E}\ dE \tag{6.2}$$

It is crucial to know the energy which neutrons have when they are selected as part of the thermal distribution. Therefore, in Figure 6.22 the normalized histogram of all 1009106 neutrons that are selected as part of the thermal population between steps number 2000 and 2100 is presented, as well as the target that caused the scattering and put the neutron in the thermal region. The thermal distribution is superimposed to the histogram as a reference. The population presented in Figure 6.22 will be further referenced as the control population.

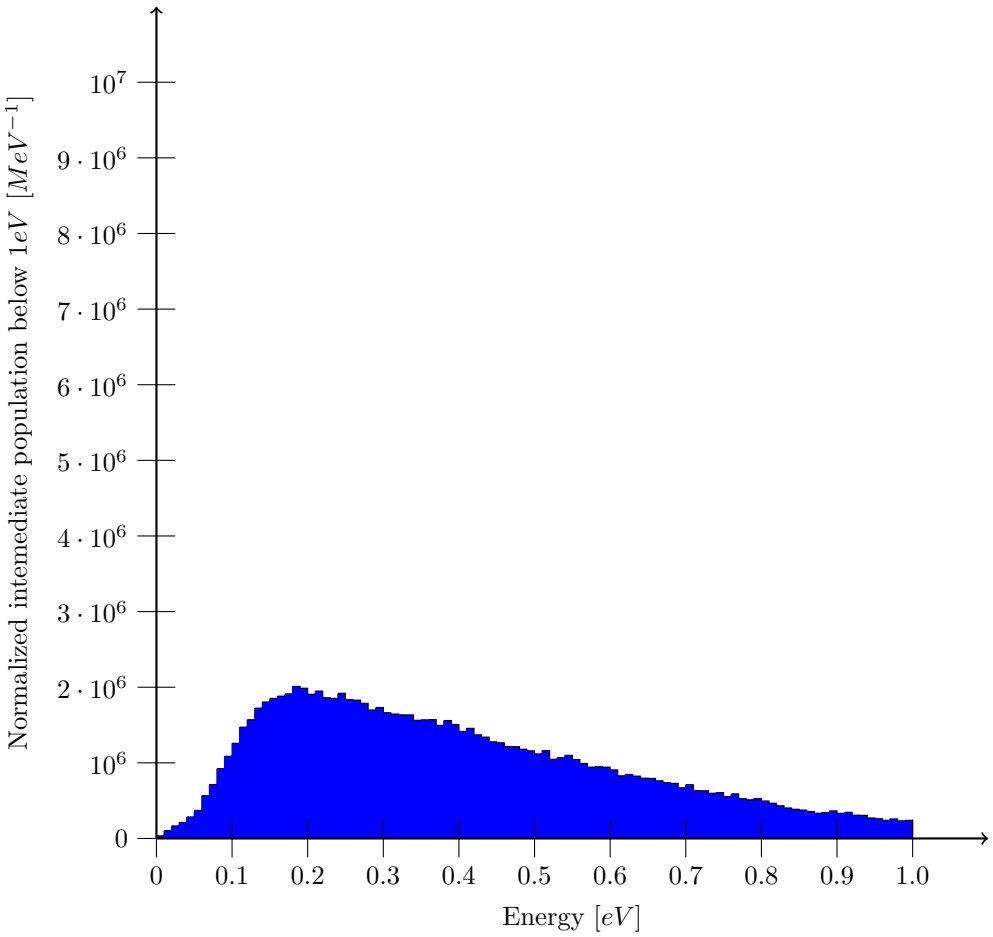

Figure 6.17 – Intermediate population spectrum in the first energy interval for step 2000.

Note that there is a discontinuity on the vertical axis, to provide a better visualization.

In the histograms of Figure 6.22 two peaks can be identified, one below the energy of 0.01 eV, and another around 0.1 eV. This is a consequence of the hypothesis that the target atoms and molecules have zero kinetic energy in the laboratory system. The occurrence of the peak below 0.01 eV is due to the collision with a hydrogen-1 atom (referred as *light target* in Figure 6.22), for the down-scattering with a particle of equal mass can bring the neutron to a halt. The presence of the second peak around 0.1 eV is related to the down-scattering of neutrons by oxygen-16 or a water molecule (referred as *medium targets* in Figure 6.22), in which more scattering reactions are needed to slow down the neutron. Heavy targets, such as uranium-235, uranium-238 and the uranium dioxide molecules, have less importance.

The mean energy of both the thermal neutrons population and the control population, can be computed by a Riemann sum based on the mid-point of each bin. For step

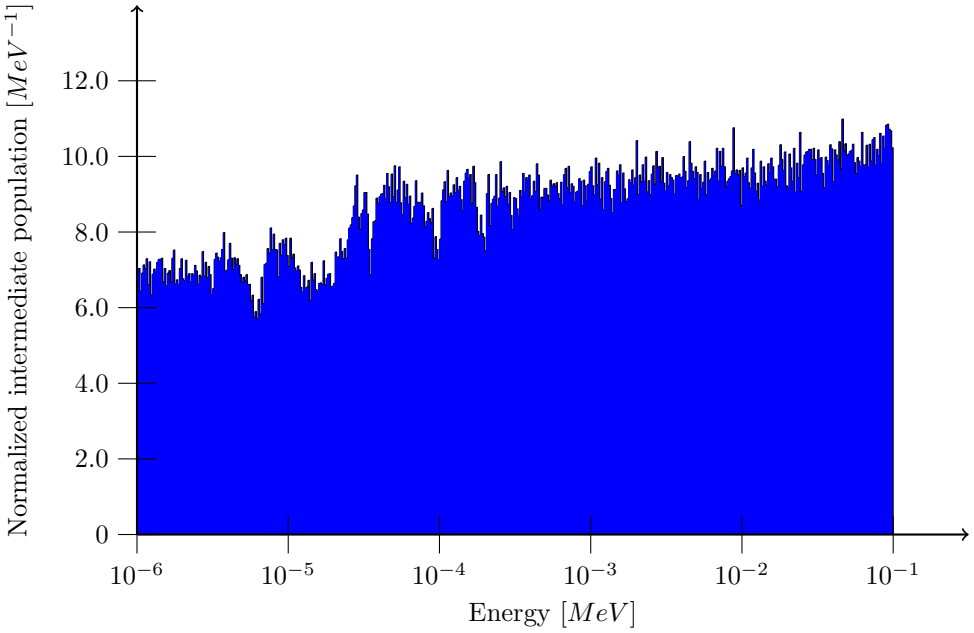

Figure 6.18 – Intermediate population spectrum in the second energy interval for step 2000.

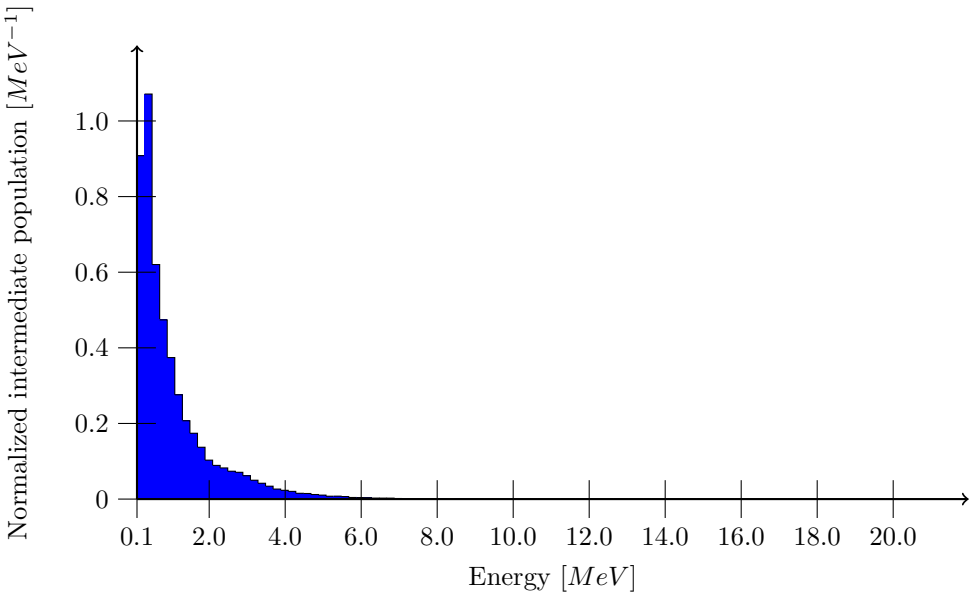

Figure 6.19 – Intermediate population spectrum in the third energy interval for step 2000.

2000 the thermal population mean energy is $7.53 \times 10^{-8}\ MeV$, comparing this to the mean energy of the control population between steps 2000 and 2100, which is $7.23 \times 10^{-8}\ MeV$, it is possible to asses the increment of kinetic energy in the neutron population, due to the simulation of up-scattering. The mean kinetic energy of the Maxwell-Boltzmann distribu-

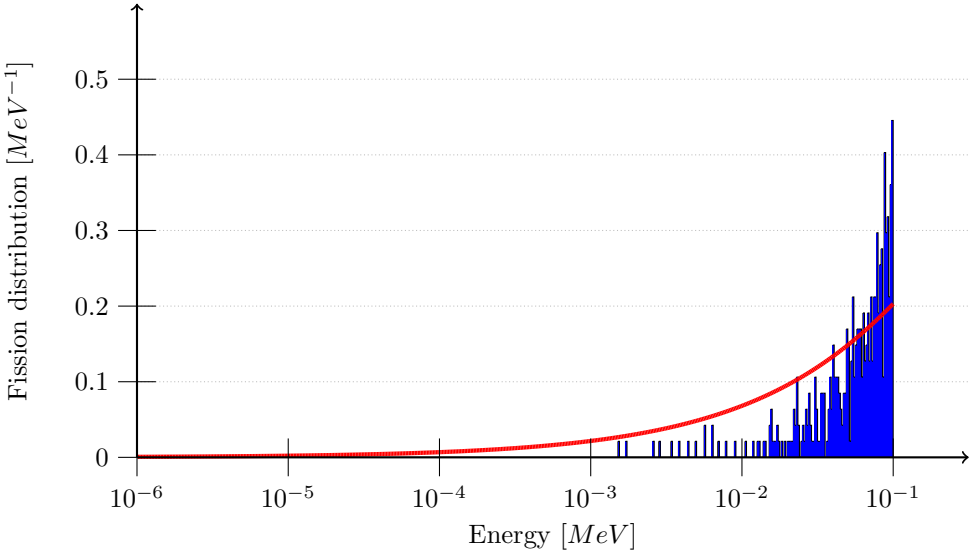

Figure 6.20 – Fission population spectrum in the second energy interval for step 2000.

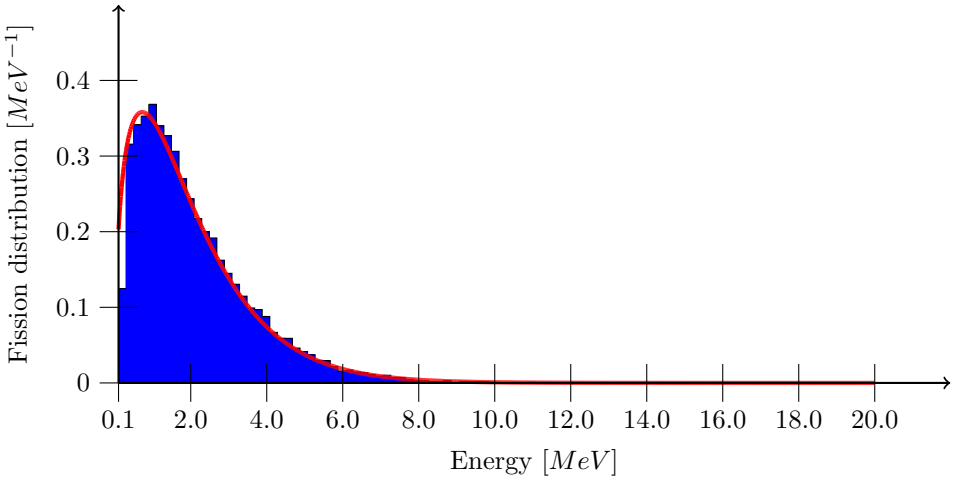

Figure 6.21 – Fission population spectrum in the third energy interval for step 2000.

tion is given by $k_B\,T\,3/2 = 7.57 \times 10^{-8}$, in which T is the temperature in K and k_B is the Boltzmann constant in MeV/K.

The neutron spectrum was also evaluated at Monte Carlo step number 3500, which has 633317 neutrons, these being 90690 thermal neutrons, 514741 neutrons that belong to the intermediate distribution, and 27886 neutrons in the fission distribution. The shape of the normalized spectra are very similar, apart from some statistical fluctuations. This results is paramount in the definition of a recurrent regime.

The spectrum of the control population was also evaluated between steps 3500 and

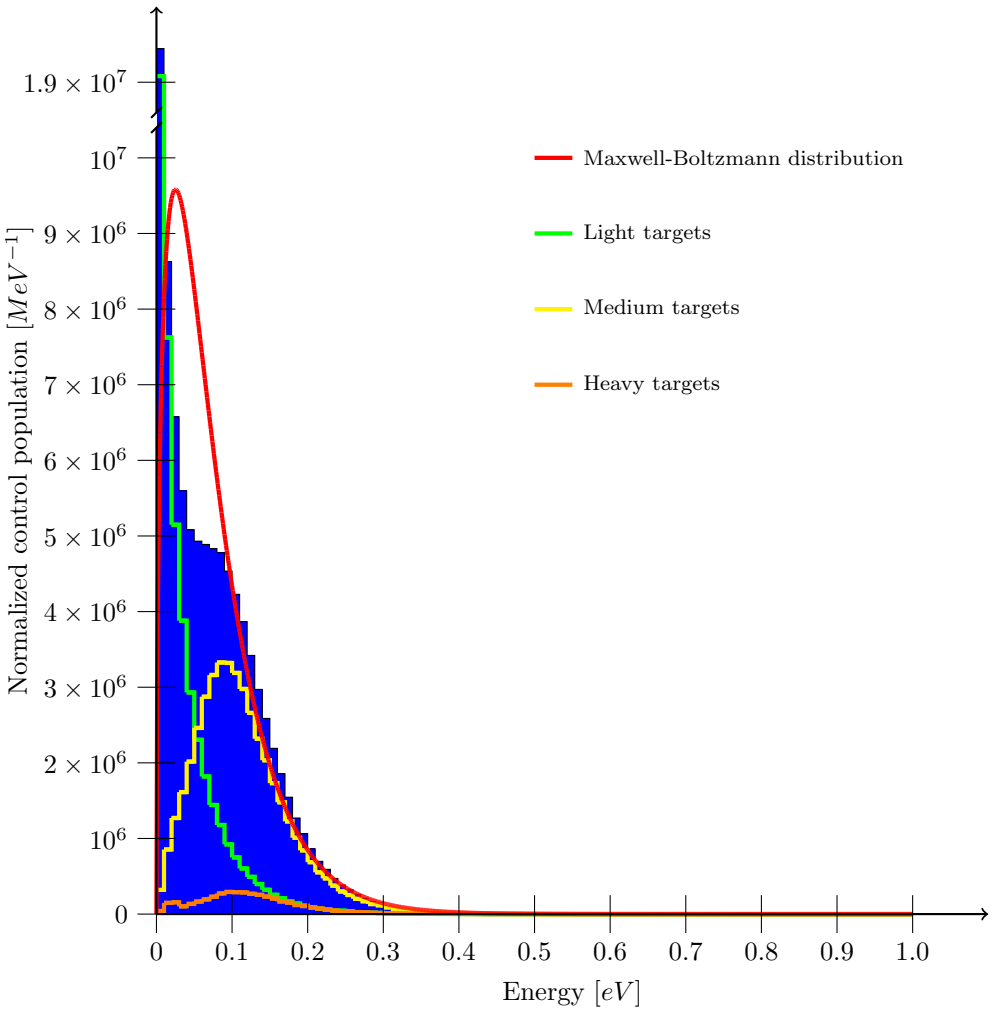

Figure 6.22 – Spectrum of thermal neutrons between steps 2000 and 2100.

3600, showing the same behaviour as the control population between steps 2000 and 2100. The Riemann sum to evaluate the mean kinetic energy of the thermal population was conducted and return a mean energy of $7.54 \times 10^{-8}\ MeV$, as well as $7.21 \times 10^{-8}\ MeV$ for the mean energy of the control population between steps 3500 and 3600. These results are very similar to the ones previously achieved.

7. CONCLUSIONS

In this work the neutron transport in reactor core material was simulated in a continuous Monte Carlo program for a starting population of 10^6 neutrons. This new procedure that implements a statistical treatment of up-scattering represents an improvement in relation to previous versions of the program, in which the main objective was the implementation of the continuous parametrization of the cross sections of H-1, O-16, U-235 and U-238.

In this endeavour the neutron population was divided in three distributions, two with fixed shape, and a third that was allowed to vary with time. These two fixed shape distributions are the thermal Maxwell-Boltzmann distributions, for slow neutrons, and the prompt fission distribution, for high energy neutrons. The third distribution is free to change its shape and it contains all neutrons that are not part of the other two. Apart from shape, the population of neutrons in all distributions can vary with time. All results were attained for all populations, the total, thermal, intermediate and fission ones.

The transient behaviour of the neutron populations was found. Also a pseudo-permanent behaviour, i.e. a recurrent regime that oscillates stochastically around a well defined mean, is found for the ratios of each distribution population to the total and also for the mean time duration of each Monte Carlo step of each population.

The spectrum of each population was shown in the form of histograms. These results are essential make the definition of a recurrent regime possible, for, although this can be perceived in the graphics of figures 6.1 to 6.11, it must be validated from the fact that the shape of each distributions also has a well defined mean behaviour. To this end, the similarity of the results attained for both steps number 2000 and 3500 is an indicative that the neutron spectrum has achieved a recurrent regime along the Monte Carlo steps, after the initial fission bias is gone.

The effects of up-scattering were simulated statistically, by correcting the spectrum of thermal neutrons. This was done by identifying the thermal neutrons, and then sampling a new energy for these neutrons from the Maxwell-Boltzmann distribution. This procedure was, as previously shown, successful in increasing the mean energy of the thermal end of the spectrum. It is also possible to perceive the hardening of the neutron spectrum, due to fission and radiative capture reactions.

Another implementation that was made in the program was the allowance for the use of any angular distribution for the scattering reactions. Previously, only isotropic scattering was considered.

One future possibility is to implement the developed program in the structure of GEANT, in order to make use of its geometry modules. Making thus possible to simulate complex geometries.

It is planned to use the developed program in a hybrid stochastic-analytical method, in which the shape of the neutron spectrum and the reaction rates are defined by Monte Carlo. Then this can be used as parameters for analytic solutions, making then use of the low computational cost of analytic methods, and the fact that the stochastic method can straightforwardly handle complex boundary conditions or complex geometry. Therefore, this work represents an important step in the direction of a versatile tool for neutral particles transport.

BIBLIOGRAPHICAL REFERENCES

Agostinelli, S.; Allison, J.; Amako, K. a.; Apostolakis, J.; Araujo, H.; Arce, P.; Asai, M.; Axen, D.; Banerjee, S.; Barrand, G. et al. Geant4—a simulation toolkit, **Nuclear instruments and methods in physics research section A: Accelerators, Spectrometers, Detectors and Associated Equipment**, vol. 506(3), p. 250–303, 2003.

Barcellos, L. F. F.; Bodmann, B. E.; Leite, S. Q. B.; de Vilhena, M. T. A Monte Carlo Simulation of a Simplified Reactor by Decomposition of the Neutron Spectrum into Fission, Intermediate and Thermal Distributions, **Annals of International Nuclear Atlantic Conference 2015**, 2015.

Bell, G. I.; Glasstone, S. **Nuclear Reactor Theory.** Technical report, Division of Technical Information, US Atomic Energy Commission, 1970.

Both, J.; Mazzolo, A.; Peneliau, Y.; Petit, O.; Roesslinger, B. **User manual for version 4.3 of the Tripoli-4 Monte-Carlo method particle transport computer code**. Technical report, 2003.

Cowan, P.; Dobson, G.; Martin, J. Release of MCBEND 11, **Proc. 12th International Conference on Radiation Shielding (ICRS-12) and 17th Topical Meeting on Radiation Protection and Shielding (RPSD-2012)**, 2013.

de Camargo, D. Q. **Um Modelo Estocástico de Simulação Neutrônica Considerando o Espectro e Propriedades Nucleares com Dependência Contínua de Energia**. PhD thesis, Universidade Federal do Rio Grande do Sul, 2011.

de Camargo, D. Q.; Bodmann, B. E.; de Vilhena, M. T.; de Queiroz Bogado Leite, S.; Alvim, A. C. M. A stochastic model for neutrons simulation considering the spectrum and nuclear properties with continuous dependence of energy, **Progress in Nuclear Energy**, vol. 69, p. 59 – 63. Research & amp; Developments in Advanced Nuclear Reactors, 2013.

Duderstadt, J.; Martin, W. **Transport Theory**. Wiley-Interscience Publications. Books on Demand, 1979.

Glasstone, S.; Sesonske, A. **Nuclear reactor engineering: Reactor design basics. Volume One**. Chapman and Hall, New York, NY (United States), 1994.

Lamarsh, J. **Introduction to nuclear reactor theory**. Addison-Wesley series in nuclear engineering. Addison-Wesley Pub. Co., 1966.

Leppänen, J. Serpent–a continuous-energy Monte Carlo reactor physics burnup calculation code, **VTT Technical Research Centre of Finland**, vol. 4, 2013.

Marsaglia, G. A current view of random number generators, **Computer Science and Statistics, Sixteenth Symposium on the Interface**, pages 3–10, 1985.

Matsumoto, M.; Nishimura, T. Mersenne Twister: A 623-dimensionally Equidistributed Uniform Pseudo-random Number Generator, **ACM Trans. Model. Comput. Simul.**, vol. 8(1), p. 3–30, 1998.

Petrie, L.; Cross, N. **KENO IV: An improved Monte Carlo criticality program**. Technical report, Oak Ridge National Lab., Tenn.(USA), 1975.

Reuss, P. **Neutron Physics**. Nuclear engineering. EDP Sciences, 2008.

Romano, P. K.; Forget, B. The OpenMC Monte Carlo particle transport code, **Annals of Nuclear Energy**, vol. 51, p. 274–281, 2013.

Sekimoto, H. **Nuclear Reactor Theory**. Tokyo Institute of Technology, 2007.

Sjenitzer, B. L. **The Dynamic Monte Carlo Method for Transient Analysis of Nuclear Reactors**. TU Delft, Delft University of Technology, 2013.

Sunny, E.; Brown, F.; Kiedrowski, B.; Martin, W. Temperature effects of resonance scattering for epithermal neutrons in MCNP, **Proc. PHYSOR–Advances in Reactor Physics–Linking Research, Industry, and Education**, pages 15–20, 2012.

Team, X.-. M. C. **MCNP: A general Monte Carlo N-Particle transport code**, 2003.

APPENDIX

Mersenne Twister Copyright Disclaimer